AD NUMBER

AD834725

LIMITATION CHANGES

TO:

Approved for public release; distribution is unlimited.

FROM:

Distribution authorized to U.S. Gov't. agencies and their contractors; Critical Technology; MAY 1968. Other requests shall be referred to Air Force Technical Application Center, VELA Seismological Center, Washington, DC 20333. This document contains export-controlled technical data.

AUTHORITY

usaf ltr, 28 feb 1972

AN ANALYSIS OF A TECHNIQUE FOR THE GENERATION OF HIGH RESOLUTION WAVENUMBER SPECTRA

23 May 1968

Prepared For

AIR FORCE TECHNICAL APPLICATIONS CENTER
Washington, D. C.

By

P. R. Lintz

TELEDYNE, INC.

Under

Project VELA UNIFORM

Sponsored By

ADVANCED RESEARCH PROJECTS AGENCY
Nuclear Test Detection Office
ARPA Order No. 624

AN ANALYSIS OF A TECHNIQUE FOR THE GENERATION OF HIGH RESOLUTION WAVENUMBER SPECTRA

SEISMIC DATA LABORATORY REPORT NO. 218

AFTAC Project No.:	VELA T/6702
Project Title:	Seismic Data Laboratory
ARPA Order No.:	624
ARPA Program Code No.:	8F10
Name of Contractor:	TELEDYNE INDUSTRIES, INC.
Contract No.:	F 33657-68-C-0945
Date of Contract:	2 March 1968
Amount of Contract:	$ 1,251,000
Contract Expiration Date:	1 March 1969
Project Manager:	Royal A. Hartenberger (703) 836-7647

P. O. Box 334, Alexandria, Virginia

AVAILABILITY

This research was supported by the Advanced Research Projects Agency, Nuclear Test Detection Office, under Project VELA-UNIFORM and accomplished under the technical direction of the Air Force Technical Applications Center under Contract F 33657-68-C-0945

TABLE OF CONTENTS

LIST OF FIGURES

LIST OF FIGURES

ABSTRACT

In this report, we discuss a method of obtaining a high-resolution wavenumber spectrum of time series data obtained from a seismic array. We derive the theoretical high-resolution wavenumber spectrum of both a single plane-wave event and an event made up of the sum of two plane waves of different amplitudes. We then process the two theoretical events and analyze the results. The plane waves for both events are simulated by impulses, with time delays between sensors chosen to simulate move out across the array. We also process the LONG SHOT event.

We conclude that although the high-resolution wavenumber spectrum does indeed give better resolution than the ordinary wavenumber spectrum, the high-resolution technique does not do a much better job of detecting a small signal in the presence of a large signal than the ordinary wavenumber spectrum. It appears that the problems of detecting a small signal in the presence of a large signal might be approached by designing an "approximate" k-space whitening filter in the time domain to "pre-whiten" the data in k-space, and then to proceed with ordinary or high-resolution frequency-wavenumber analysis.

INTRODUCTION AND THEORY

Frequency-wavenumber spectra

The ordinary three dimensional frequency-wavenumber spectrum (Burg, 1964) of time series data sampled at discrete points in space is given by:

$$P(f,\underset{\sim}{k}) = \sum_{j=1}^{N} \sum_{m=1}^{N} S_{jm}\,(\omega,\underset{\sim}{x}_{jm}) \exp\left[-i2\pi\ \underset{\sim}{k} \cdot (\underset{\sim}{x}_j - \underset{\sim}{x}_m)\right]$$

where S_{jm} is the $jm^{\underline{th}}$ element of the spectral matrix. The fact that $P(f,\underset{\sim}{k})$ is real can be seen by writing it as:

$$P(f,\underset{\sim}{k}) = \sum_{j=1}^{N} S_{jj}\,(\omega) + 2 \sum_{j=2}^{N} \sum_{m=1}^{N} |S_{jm}(\omega)|$$

$$\cos\left[2\pi\ \underset{\sim}{k} \cdot (\underset{\sim}{x}_j - \underset{\sim}{x}_m) - (\theta_j - \theta_m)\right] \quad ;m<j$$

where

$$\theta_j - \theta_m = \omega\ \left[\tau_j\,(\omega) - \tau_m\,(\omega)\right] = 2\pi\ \underset{\sim}{k}_o \cdot (\underset{\sim}{x}_j - \underset{\sim}{x}_m)$$

It is convenient to write the ordinary frequency-wavenumber spectrum in vector notations as:

$$P(f,\underset{\sim}{k}) = \underset{\sim}{\Delta}^{+}\ S\ \underset{\sim}{\Delta}$$

where

$$\underset{\sim}{\Delta}^{+} = \left[\exp\,(-i2\pi\ \underset{\sim}{k} \cdot \underset{\sim}{x}_1),\ \exp\,(-i2\pi\ \underset{\sim}{k} \cdot \underset{\sim}{x}_2) \cdots \exp\,(-i2\pi\ \underset{\sim}{k} \cdot \underset{\sim}{x}_m)\right]$$

is a row vector, the hermitian conjugate of $\underset{\sim}{\Delta}$ and where S is the N x N spectral matrix:

$$S = \begin{bmatrix} S_{11} & S_{12} & \cdots & S_{1N} \\ S_{12}^{*} & S_{22} & \cdots & S_{2N} \\ \cdot & \cdot & & \\ \cdot & \cdot & & \\ \cdot & \cdot & & \\ S_{1N}^{*} & S_{2N}^{*} & \cdots & S_{NN} \end{bmatrix}$$

The technique of computing high-resolution wave-number spectra follows the method used by Haney, (1967). The basic method consists of designing a multichannel filter whose desired output is an impulse at time $t = t_o$ and spatial lag $x = x_o$, where t_o is usually zero and x_o is the spatial position of one of the seismometers. This method, then, consists of designing a least-mean-square error "whitening" filter to "whiten" the data in f-k space. The inverse of the f-k response of the filter which gives a "white" or constant f-k spectrum when applied to the space-time series data should give a good estimate of the true f-k spectrum of the original data. This method could also be considered as equivalent to extending the spatial correlation functions (Burg, 1967).

The multichannel whitening filter is sensitive to gain inequalities. One method of compensation is to normalize the spectral matrix (Haney, 1967):

$$S_{ij} = \frac{S_{ij}}{S_{ii}\, S_{jj}} = \sigma_{ij} \exp\,(i\theta_{ij})$$

where σ_{ij} is the ordinary coherence between channel i and channel j and θ_{ij} is the phase difference between channel i and channel j. Thus the normalized spectral matrix is

$$\begin{bmatrix} 1.0 & \sigma_{12} \exp\,(i\theta_{12}) & \cdots & \sigma_{1N} \exp\,(i\theta_{1N}) \\ \sigma_{12} \exp\,(-i\theta_{12}) & 1.0 & & \cdot \\ \cdot & \cdot & & \cdot \\ \cdot & \cdot & & \cdot \\ \cdot & \cdot & & \\ \sigma_{1N} \exp\,(-i\sigma_{1N}) & \sigma_{2N} \exp\,(-i\theta_{2N}) & \cdots & 1.0 \end{bmatrix}$$

All the information concerning velocity and azimuth is included in the coherence and phase, so normalizing the spectral matrix at each frequency cannot change the apparent velocity and azimuth of an event. Using the normalized spectral matrix, the multichannel filter design equations become:

$$(cI + S)\ (\underset{\sim}{m}_H) = \underset{\sim}{m}_U$$

where

$$\underset{\sim}{m}_U^+ = \left[0, 0, \cdots 1, \ 0, \ 0, \cdots \ 0\right]$$

or

$$\underset{\sim}{m}_U = \underset{\sim}{\delta}_{im}$$

The high-resolution f-k spectrum designed on the mth sensor is given by:

$$m_P\ (f, \underset{\sim}{k}) = \left(\underset{\sim}{\Delta}^+ \overline{m_H\ m_H^+}\ \underset{\sim}{\Delta} \right)^{-1}$$

$$m_H = (cI + S)^{-1}\ m_U = Q\ m_U$$

where m_U is a vector which picks out the mth column of any matrix by which it is multiplied. Thus

$$\overline{m_H\ m_H^+} = \overline{m_Q\ m_Q^+} = \overline{m_Q^2}$$

The spectrum of an impulse at time t=o and position $x = x_o$ and $x = o$ is

$$\left[2 + 2 \cos\ (2\pi\ \underset{\sim}{k} \cdot \underset{\sim}{x}_o)\right]$$

This function has a maximum value along lines perpendicular to x_o and spaced at intervals in $\underset{\sim}{k}$ space of $k = n/x_o$. The net result of designing a high resolution f-k spectrum on sensors not at the origin but as some $\underset{\sim}{x} = \underset{\sim}{x}_o$ will result in a non-physically meaningful stretching of the f-$\underset{\sim}{k}$ spectrum along a line perpendicular to $\underset{\sim}{x}_o$. However, calculating the f-k spectrum over all of the sensors in the array is useful since effects such as seismometer response and ground coupling tend to cancel out and the non-physically-meaningful stretching of the f-k spectrum also tends to cancel out for symmetric arrays.

The average spectral matrix of the whitening filters designed on each of the sensors in turn is

$$\frac{1}{N} \sum_{m=1}^{N} \overline{m_H \, m_H^+} = \frac{Q^2}{N}$$

The quantity Q^2 is very easy to calculate, since it is the square of the inverse of some constant times the identity matrix plus the smoothed spectral matrix. The constant (c) can be considered to be the signal-to-noise ratio of the random signal spectral matrix I.

Response of the high-resolution technique to a single plane wave input

In the special case of an impulsive plane wave with unity coherence between sensors, the spectral matrix may be factored as follows:

$$S = \underset{\sim}{u} \, \underset{\sim}{u}^+$$

where $\underset{\sim}{u}^+$ is the row vector

$$\left[\exp(-i\omega\tau_1), \exp(-i\omega\tau_2), \cdots \exp(-i\omega\tau_2)\right]$$

but

$$(cI + uu^+)^{-1} = \frac{1}{c}\left(I - \frac{u\,u^+}{c+u^+u}\right) = Q$$

and $u^+ u = N$
so that

$$Q^2 = \frac{1}{c^2}\left[I - \frac{uu^+}{c+N}\left(2 - \frac{N}{c+N}\right)\right]$$

Since $\underset{\sim}{\Delta}^+ I \underset{\sim}{\Delta} = N$

$$\underset{\sim}{\Delta}^+ Q^2 \underset{\sim}{\Delta} = \frac{1}{c^2}\left[N - \frac{\underset{\sim}{\Delta}^+ u\,u^+ \underset{\sim}{\Delta}}{c+N}\left(2 - \frac{N}{c+N}\right)\right]$$

$$\underset{\sim}{\Delta}^+ u\,u^+ \underset{\sim}{\Delta} = P(f,\underset{\sim}{k}) = \text{ordinary f-k spectrum}$$

$(c+N)^{-1}$ may be expanded for $c<N$ as follows:

$$\Phi HR(f,k) = \frac{N}{\underset{\sim}{\Delta}^+ Q^2 \underset{\sim}{\Delta}} = \frac{c^2 N}{\left[N - \frac{P(f,k)}{N}\left(1 - \left(\frac{c}{N}\right)^2 + 3\left(\frac{c}{N}\right)^3 - 4\left(\frac{c}{N}\right)^4 \cdots\right)\right]}$$

but

$$P(f,k) = \sum_{j=1}^{N} S'_{jj}(\omega) + 2 \sum_{\substack{j=2 \\ m<j}}^{N} \sum_{m=1}^{N} |S'_{jm}(\omega)| \cos \left[2\pi \, (\underset{\sim}{k}-\underset{\sim}{k}_o)\cdot(\underset{\sim}{x}_j-\underset{\sim}{x}_m) \right]$$

at $\underset{\sim}{k} = \underset{\sim}{k}_o$

$$P(f,\underset{\sim}{k}) = P_{max} = N + 2C_2^N = N + 2 \left[\frac{N(N-1)}{2} \right] = N^2$$

Thus

$$\Phi HR \, (f,\underset{\sim}{k}_o) \simeq \frac{c^2 N}{N - N\left[1 - \left(\frac{c^2}{N}\right)\right]} = N^2$$

hence the maximum value of $\Phi HR(f,\underset{\sim}{k})$ is independent of c up to terms of the order $\left(\frac{c}{N}\right)^3$,

when

$$P(f,\underset{\sim}{k}) \to 0$$

$$\Phi HR(f,\underset{\sim}{k}) \to c^2$$

Response of the high resolution technique to an input consisting of two plane waves input

In the case of where the event consists of two plane waves of unity coherence, one wave of amplitude unity, the other of amplitude b, the ordinary f-k spectrum is:

$$P(f,\underset{\sim}{k}) = \underset{\sim}{\Delta}^+ (u_1 + bu_2) \, (u_1^+ + bu_2^+) \, \underset{\sim}{\Delta}$$

$$P(f,\underset{\sim}{k}) = \underset{\sim}{\Delta}^+ \, u_1 \, u_2^+ \, \underset{\sim}{\Delta} + b^2 \, \underset{\sim}{\Delta}^+ \, u_2 \, u_2^+ \, \underset{\sim}{\Delta} + b \, \underset{\sim}{\Delta}^+ \, (u_1 \, u_2^+ + u_2 \, u_1^+) \, \underset{\sim}{\Delta}$$

Let

$$\frac{1}{2}\,(u_1\,u_2^{+} + u_2\,u_1^{+}) = G(\omega)$$

then

$$P(f,\underset{\sim}{k}) = P,(f,\underset{\sim}{k}) + b^2\,P_2(f,\underset{\sim}{k}) + 2b\,\underset{\sim}{\Delta}^{+}\,G(\omega)\,\underset{\sim}{\Delta}$$

where

$$G_{ij}(\omega) = \cos\left[2\pi f(t_i' - t_j)\right]$$

where t_i' is the arrival time of plane wave number 1 at sensor i and t_j is the arrival time of plane wave number 2 at sensor j.

For the high-resolution frequency-wavenumber spectrum,

$$\left[cI + (u_1 + bu_2)\right]^{-1} = Q = \frac{1}{c}\left[I - \frac{(u_1 + bu_2)\,(u_1^{+} + bu_2^{+})}{c + (u_1^{+} + bu_2^{+})\,(u_1 + bu_2)}\right]$$

$$(u_1^{+} + bu_2^{+})\,(u_1 + bu_2) = (1 + b^2)\,N + b\,(u_1^{+}\,u_2 + u_2^{+}\,u_1)$$

$$b(u_1 + u_2 + u_2^{+}\,u_1) = 2\,b\sum_{i=1}^{N}\cos\left[2\pi f\,(t_i' - t_i)\right] = 2b\,Tr\left[G(\omega)\right]$$

$$Q = \frac{1}{c}\left[I - \frac{(u_1 + bu_2)\,(u_1^{+} + bu_2^{+})}{c + R(\omega)}\right]$$

where

$$R(\omega) = (1 + b^2)N + 2b\ \mathrm{Tr}\left[G(\omega)\right]$$

$$Q^2 = \frac{1}{c^2}\left\{I - \frac{(u_1 + bu_2)(u_1^+ + bu_2^+)}{c + R(\omega)}\left[2 - \frac{R(\omega)}{c + R(\omega)}\right]\right\}$$

$$\underset{\sim}{\Delta}^+ Q^2 \underset{\sim}{\Delta} = \frac{1}{c^2}\left\{N - \frac{P(f,\underset{\sim}{k})}{c + R(\omega)}\left[2 - \frac{R(\omega)}{c + R(\omega)}\right]\right\}$$

and where

$P(f,\underset{\sim}{k})$ is the ordinary f-$\underset{\sim}{k}$ spectrum

$$P(f,\underset{\sim}{k}) = P_1(f,\underset{\sim}{k}) + b^2 P_2(f,k) + 2b\ \underset{\sim}{\Delta}^+ G(\omega)\ \underset{\sim}{\Delta}$$

$$\Phi HR(f,k) = \frac{N}{\underset{\sim}{\Delta}^+ Q^2 \underset{\sim}{\Delta}}$$

Expanding $\left[c + R(\omega)\right]^{-1}$ and simplifying, we have

$$\Phi HR(f,\underset{\sim}{k}) = \frac{c^2 N}{N - \frac{P(f,k)}{R(\omega)}\left[1 - \left(\frac{c}{R(\omega)}\right)^2 + 3\left(\frac{c}{R(\omega)}\right)^3 + \cdots\right]}$$

The expression for the high-resolution wavenumber spectrum for two plane waves input is seen to be quite similar to the expression for the spectrum of a single plane wave, with the exception that $P(f,k)$ has cross terms, and N is replaced by $R(\omega)$ in the expansion $(c + N)^{-1}$.

PROCEDURE AND RESULTS

Procedure

Synthetic spike seismograms were generated for the WMO array and for the LASA XE3 array. The WMO seismogram corresponded to a 12 km/sec impulse arriving from due south of the array. The XE3 seismogram consisted of the sum of two impulses, one from due north with an apparent horizontal velocity of 20 km/sec and an amplitude of unity, and the second impulse from due south with an apparent horizontal velocity of 30 km/sec and an amplitude of 0.2. The LONG SHOT event at LASA subarray F1 was also processed. The spectral matrix of each input was calculated and smoothed using the fast Fourier transform program of Claerbout, et al. (McCowan, 1966). Both ordinary and high-resolution spectra were calculated for each event. High-resolution spectra calculated on individual sensors and averaged over all sensors (as discussed in Section A) were generated for the single plane wave at WMO, while only the "average" high-resolution spectra were calculated for the two-wave event at LASA XE3.

The ordinary and the high-resolution f-k spectra of a single plane wave input

Figures 3 and 7 are the ordinary f-k spectrum of the 12 km/sec impulse at frequencies .3125 cps and .9375 cps. Figures 4 and 8 are the high-resolution wavenumber spectrum (designed on the center seismometer) for the same event at the same frequencies. Comparing Figure 4 with Figure 3, we see that the high-resolution wavenumber spectrum at .325 cps indeed shows an improvement in resolution over the ordinary spectrum (Figure 3). Figure 4 shows a signal arriving from the south with a velocity of slightly greater than 10 km/sec, whereas Figure 3 (the ordinary f-k spectrum) shows a signal coming from the general direction of the south but with much uncertainty as to the exact velocity and azimuth. At 0.9375 cps, the ordinary f-k spectrum (Figure 7) shows a plane wave from a southerly direction, but the amount of uncertainty as to velocity and azimuth is

large compared to that of the high-resolution spectrum (Figure 8). Figures 5 and 9 are the high-resolution wavenumber spectrum (designed on the sensor located at (.94, - .17) at frequencies .3125 cps and .9375 cps. Comparing Figure 5 with Figure 4, we see that the resolution of the high-resolution f-k spectrum (Figure 5) designed on the seismometer at (.94, - .17) is approximately equal to the resolution of the high-resolution f-k spectrum (Figure 4) designed on the center (0,0) seismometer; however, the spectrum in Figure 5 is "stretched" along the line perpendicular to the direction of the line connecting the origin to the position (.94, - .17). In other words, the direction of the stretch is $90° + \tan^{-1}(-.17/.94) = 90° - 16°$, or $\theta = 74°$. The resolution of Figure 9, the high-resolution spectrum at .9375 cps designed on the off-center seismometer is approximately equal to that of Figure 8, but again the spectrum is stretched in the direction of 74°. Thus the net result of designing a high-resolution f-k spectrum on a seismometer located at $\underset{\sim}{x} = \underset{\sim}{x}_o$ is indeed to introduce a $\cos(2\pi \underset{\sim}{k} \cdot \underset{\sim}{x}_o)$ term, which causes a stretching of the spectrum along a direction perpendicular to the vector $\underset{\sim}{x} = \underset{\sim}{x}_o$. Figures 6 and 8 are the high-resolution f-$\underset{\sim}{k}$ spectra averaged over all of the seismometers in the array, for the 12 km/sec event, at frequencies .3125 cps and .9375 cps. Comparing Figure 6 with Figures 4 and 5, we see that in the high-resolution spectrum which has been averaged over all of the seismometers, the non-physically meaningful stretching of the spectrum due to designing the high-resolution spectrum on an off-center seismometer has been cancelled out. The spectrum of Figure 5 seems to be not quite as peaked as that of Figure 4, although the difference is insignificant. The spectrum of Figure 4 is also tilted to the left due to the asymmetry of the WMO array, whereas the spectrum of Figure 5 seems to be slightly "stretched" in a northwardly direction. Figure 10 is the high-resolution wavenumber spectrum averaged over all seismometers in the array, at .9375 cps. The averaged spectrum has slightly less resolution than the spectrum that was designed on the center seismometer (Figure 8); however, the "stretching" of the spectrum

evident in the spectrum designed on the off-center seismometer (Figure 9) has essentially been cancelled out. The averaged spectrum should give better results when effects such as different seismometer responses and ground coupling for each sensor are considered.

Figures 12, 14, and 16 are the ordinary f-k spectrum of LONG SHOT recorded at LASA F1 at frequencies 0.625, 1.5625, and 2.50 cps. Figures 13, 15, and 17 are the "averaged" high-resolution f-k spectra at the same frequencies. The signal-to-noise ratio (c) was 2.0. At 0.625 cps, both the averaged high-resolution (Figure 13) and the ordinary spectrum (Figure 2) indicate the event is coming from the correct direction, but the velocity is somewhat smaller than expected (11.6 km/sec, vs 14.1 km/sec, from the J-B travel-time tables). At 1.5625 cps the high-resolution spectrum (Figure 15) shows a velocity of approximately 18 km/sec, whereas the ordinary f-k spectrum, (Figure 14) shows a velocity closer to the velocity computed from the travel-time tables, although the resolution is such as to leave a large uncertainty as to the exact velocity and azimuth. At 2.50 cps both the high-resolution (Figure 18) and the ordinary f-k spectrum (Figure 17) agree quite well as to the velocity and azimuth of LONG SHOT at LASA F1. The velocity of the event is quite close to the predicted 14.1 km/sec velocity. The high-resolution spectrum offers a little more resolution and hence less uncertainty than the ordinary f-k spectrum. Figure 18 is a beam-steered (time-shift and sum) power density spectrum of LONG SHOT. Nine seismometers in-line in the approximate direction of the event were time-shifted and summed. The power spectrum of the sum was then computed and displayed in Figure 18. This demonstrates that there is indeed enough power at 2.5 cps to give an accurate f-k spectrum at that frequency.

<u>The ordinary and the high-resolution f-k spectra of two plane waves input</u>

Figure 20 is the array response of thirteen of the seismometers at LASA XE3. Figures 21, 24, and 27 are the ordinary f-k spectrum

of a plane wave of velocity 20 km/sec and amplitude 1.0 plus a plane wave of velocity 30 km/sec and amplitude 0.2, computed at 0.625, 1.25, and 1.875 cps. Figures 22, 25, and 28 are the averaged high-resolution f-k spectrum (S/N = 2.0) of the same event calculated at the same frequencies. Figures 23, 26, and 29 are the high-resolution f-k spectrum (S/N = 0.03) of the same event, calculated at the same frequencies. At .625 cps the 30 km/sec event would not be detected by either the ordinary f-k spectrum (Figure 21) or by the average (S/N = 2.0) high-resolution f-k spectrum (Figure 22). The extreme elongation of the average (S/N = .03) high-resolution f-k spectrum (Figure 23) might make one suspicious about the presence of a second event, but the conclusion would depend on the subjective discrimination of the analyst. At 1.25 cps, neither the ordinary f-k spectrum (Figure 24) nor the averaged high-resolution (S/N = 2.0) f-k spectrum offer much possibility of detecting the 30 km/sec plane wave in the presence of the larger 20 km/sec event. The averaged high-resolution (S/N = 0.3) f-k spectrum offers a distinct possibility of detection, although the resolution of the two peaks is far from optimum. At 1.975 cps, the 30 km/sec event would probably be mistaken for a side lobe of the ordinary f-k spectrum (Figure 27). The averaged high-resolution (S/N = 2.0) f-k spectrum (Figure 28) does not give any indication of the 30 km/sec event. The averaged high-resolution (S/N = .03) f-k spectrum gives a definite indication of the smaller event, but there is a spurious 6 db peak at 10 km/sec from the southwest. The complicated spectra of an event made up of a sum of two plane waves is due to the cross-terms $\Delta^{+}G(\omega)\Delta$ in the frequency-wavenumber spectrum which give rise to spurious peaks.

CONCLUSIONS

From this report, we conclude that although the high-resolution frequency-wavenumber spectrum gives much better resolution for single events, the high-resolution technique does not improve significantly the capability of a seismic array to detect multiple time-overlapping events from different azimuths. A possible method of detecting a small event in the presence of a large event is, we suggest, to design an approximate pre-whitening filter in the time domain to approximately "whiten" the f-k spectrum of the data, convolve the filter with the time series data and then proceed with either ordinary or high-resolution f-k analysis. The fact that the pre-whitening filter need be only an approximate whitening filter would leave quite a bit of lattitude in its design.

REFERENCES

Burg, J.P., 1964, Three dimensional filtering with an array of seismometers: Geophysics, v. 29, p. 693-713.

Burg, J.P., 1967, Maximum-entropy spectral analysis: presented at the 37th annual meeting of the Society of Exploration Geophyscists.

Haney, W.P., 1967, Research on high-resolution frequency-wavenumber spectra, Special Scientific Report No. 2: Dallas, Texas Instruments, Inc., Contract AF33(657)16678.

McCowan, D.W., 1966, Finite fourier transform theory and its application to the computation of convolutions, correlations, and spectra, Technical Memorandum No. 8-66: Alexandria, Earth Sciences, A Teledyne Company.

McCowan, D.W. and Lintz, P.R., 1968, High-resolution frequency-wavenumber spectra, Seismic Data Laboratory Report No. 206, Alexandria, Virginia, Earth Sciences, A Teledyne Company.

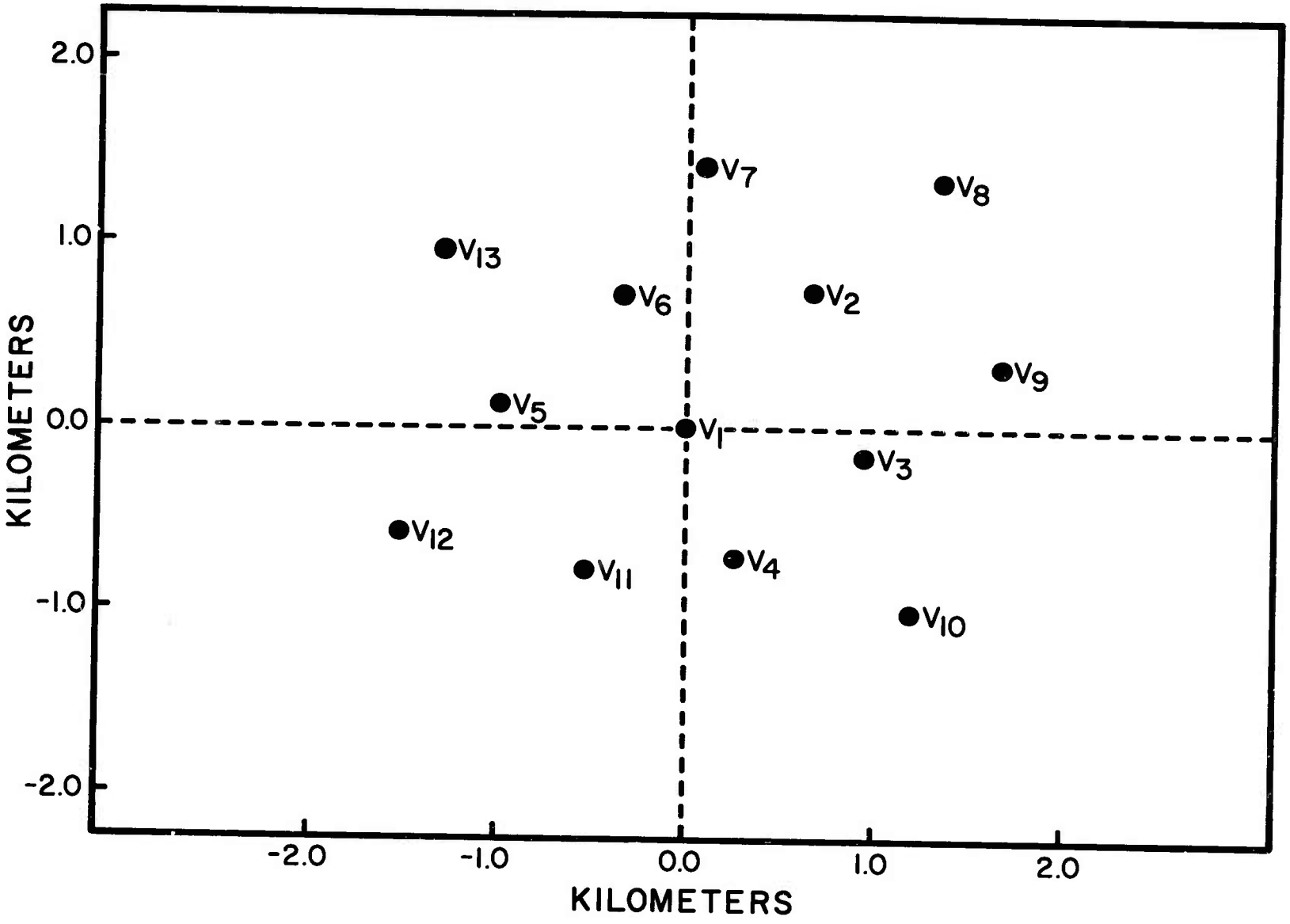

Figure 1. WMSO surface array

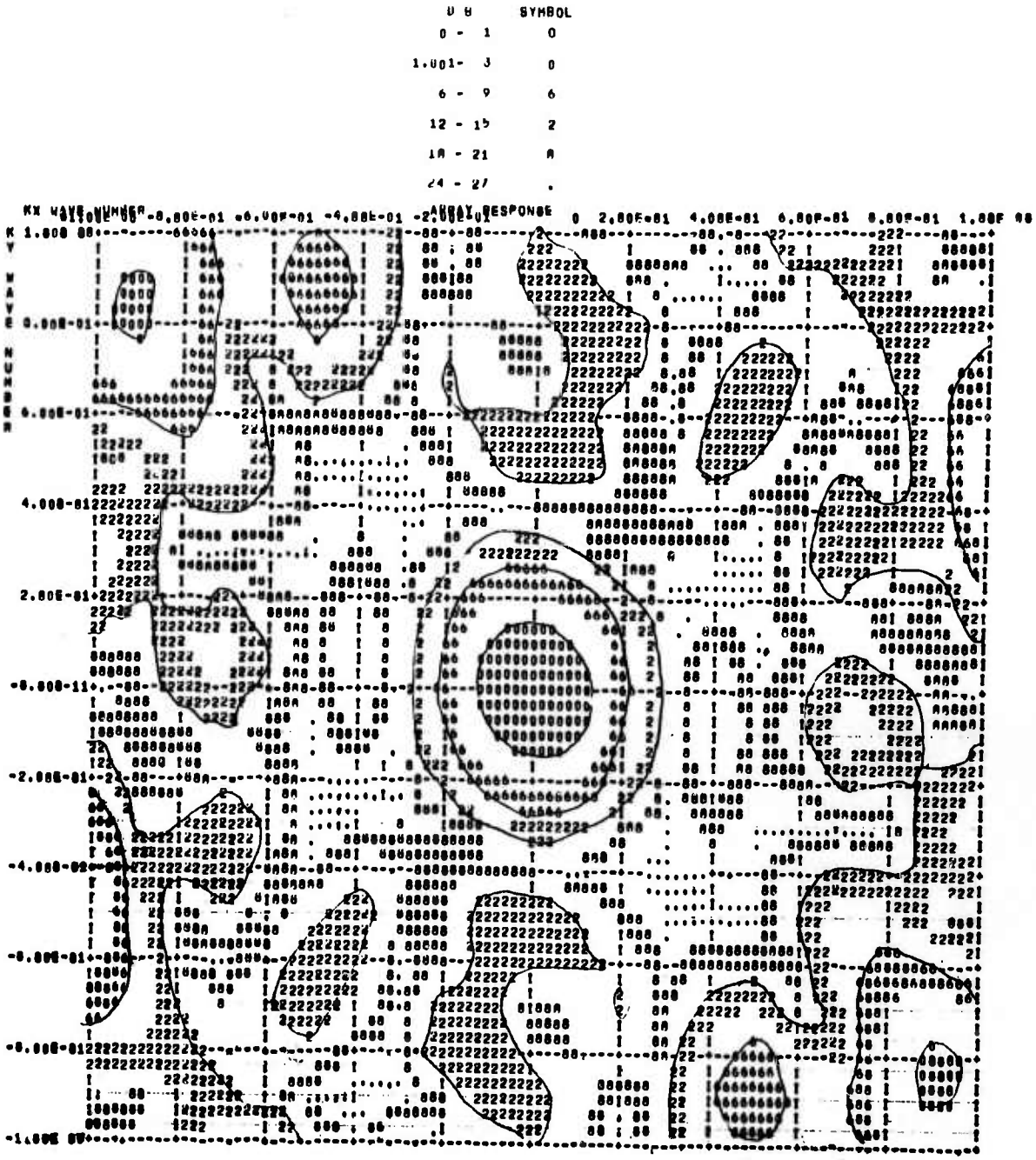

Figure 2. The WMO array response to an infinite-velocity plane wave.

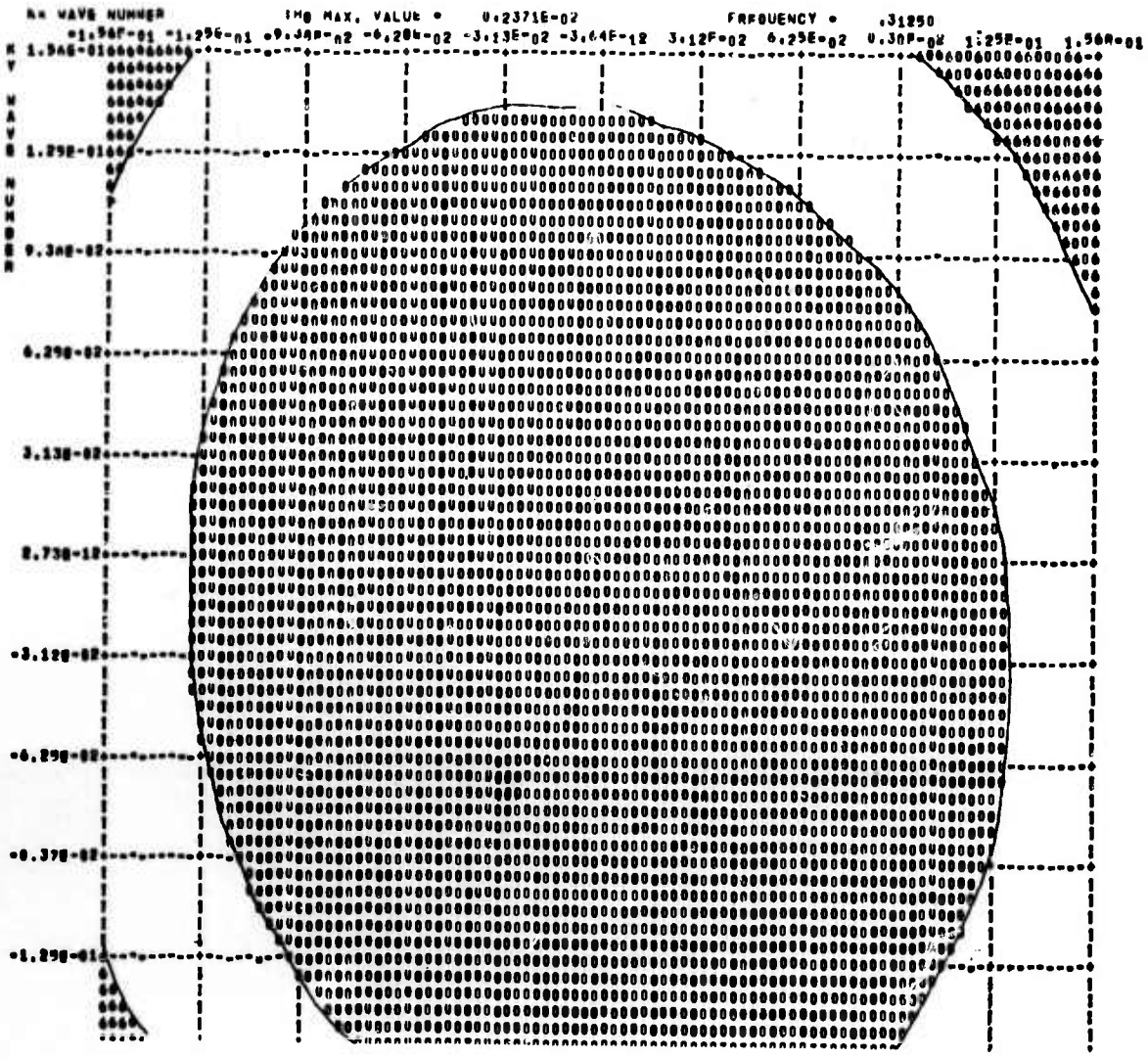

Figure 3. The ordinary f-k spectrum of a theoretical 12.0 km/sec plane wave arriving at WMO from the south; the frequency is 0.3125 cps.

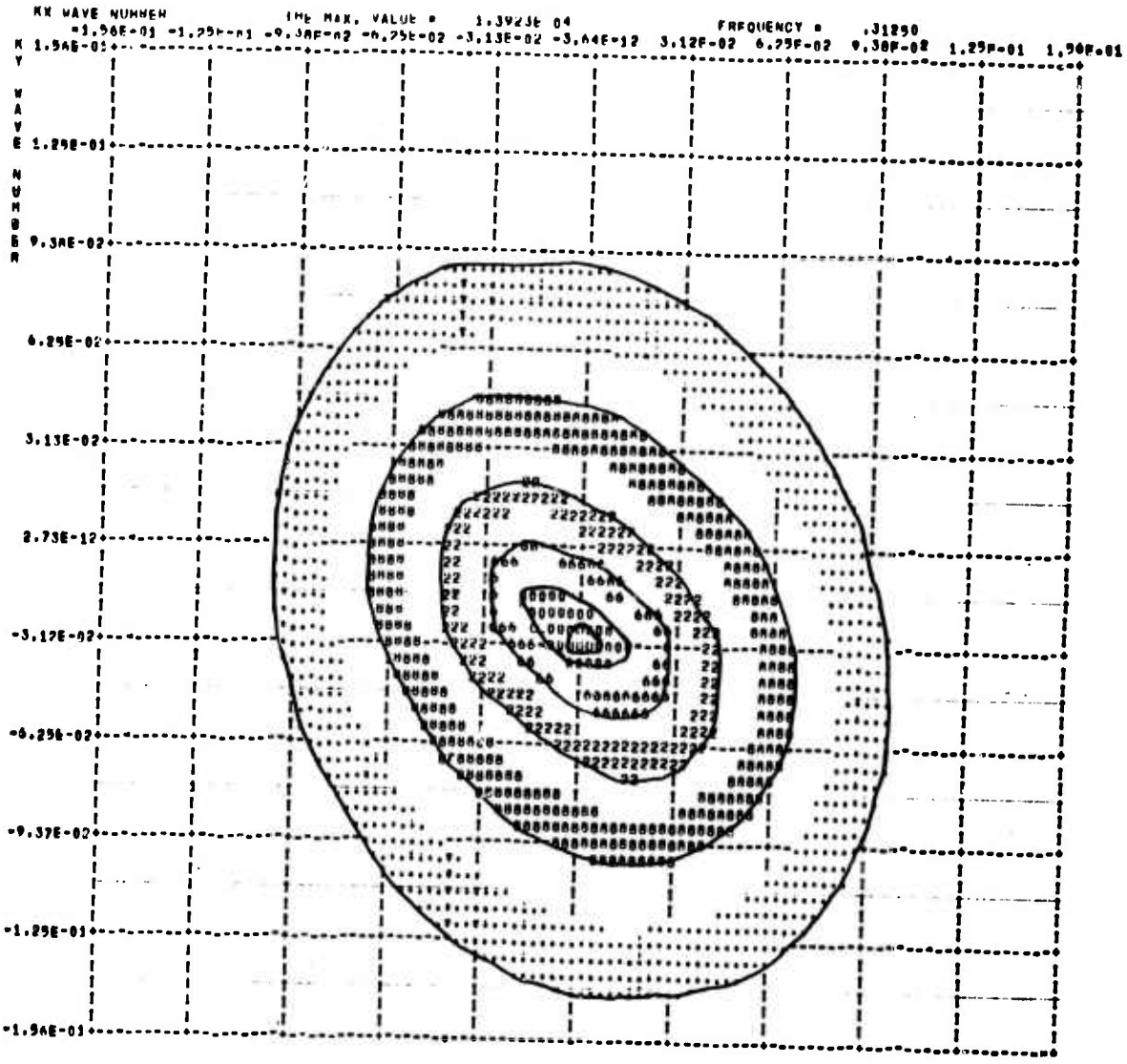

Figure 4. The high-resolution f-k spectrum of the 12.0 km/sec event at 0.3125 cps; S/N = .03.

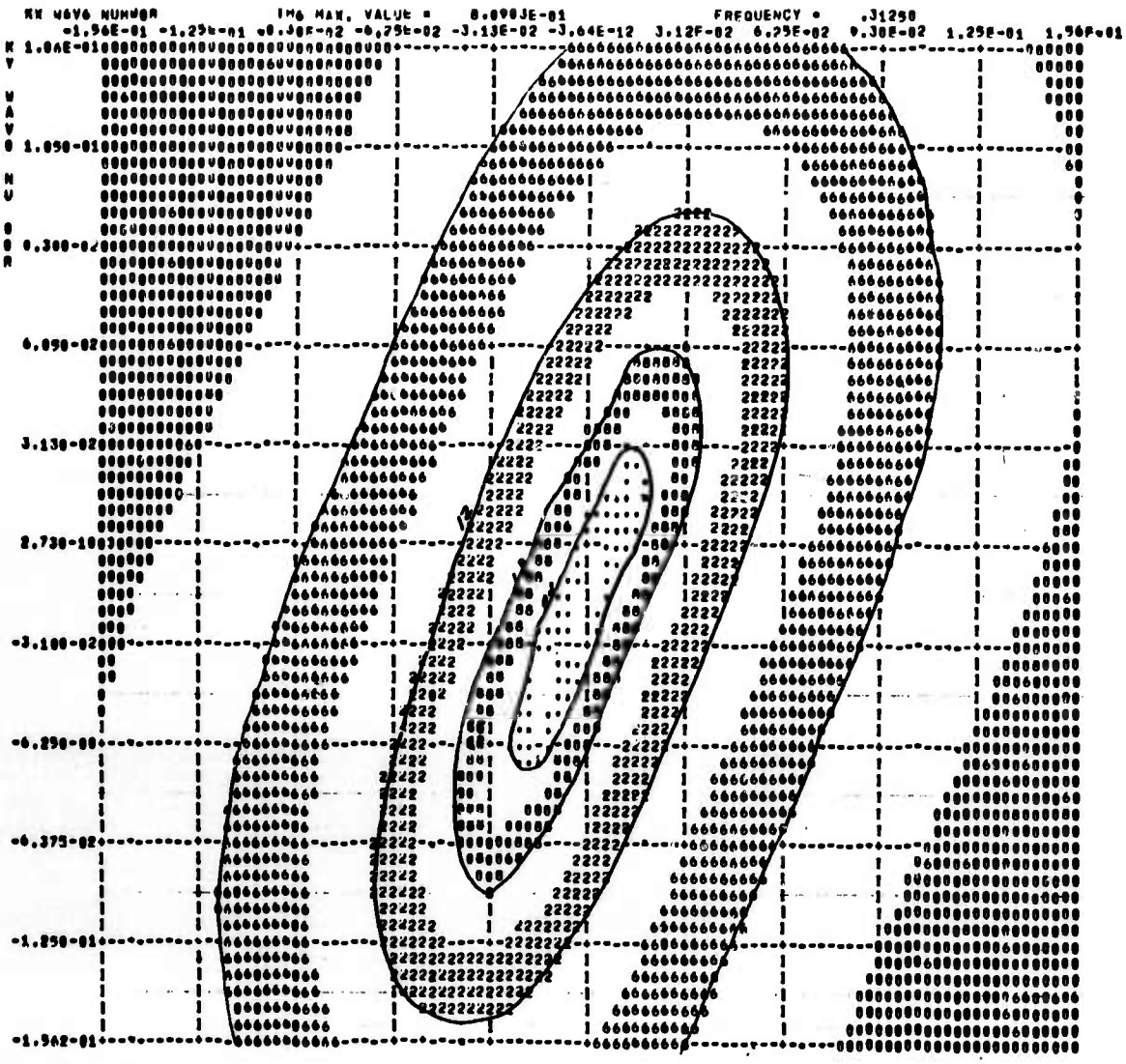

Figure 5. The high-resolution f-k spectrum for the 12.0 km/sec plane waves at frequency at 0.3125 cps. The reference seismometer is located at (.94,-.17); S/N = .03.

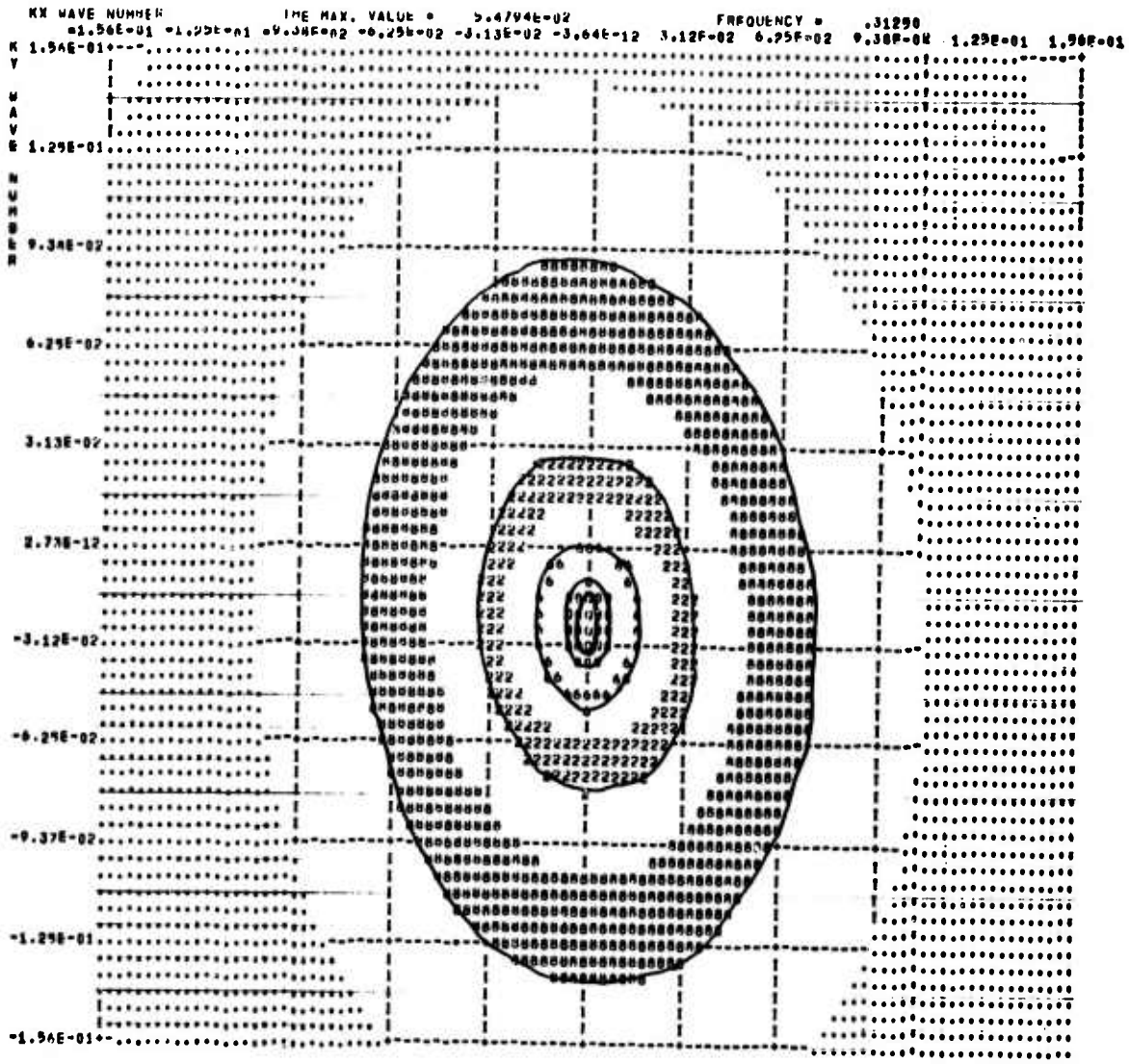

Figure 6. The high-resolution f-k spectrum for the 12 km/sec plane wave at .3125 cps averaged over all of the seismometers; S/N = .03.

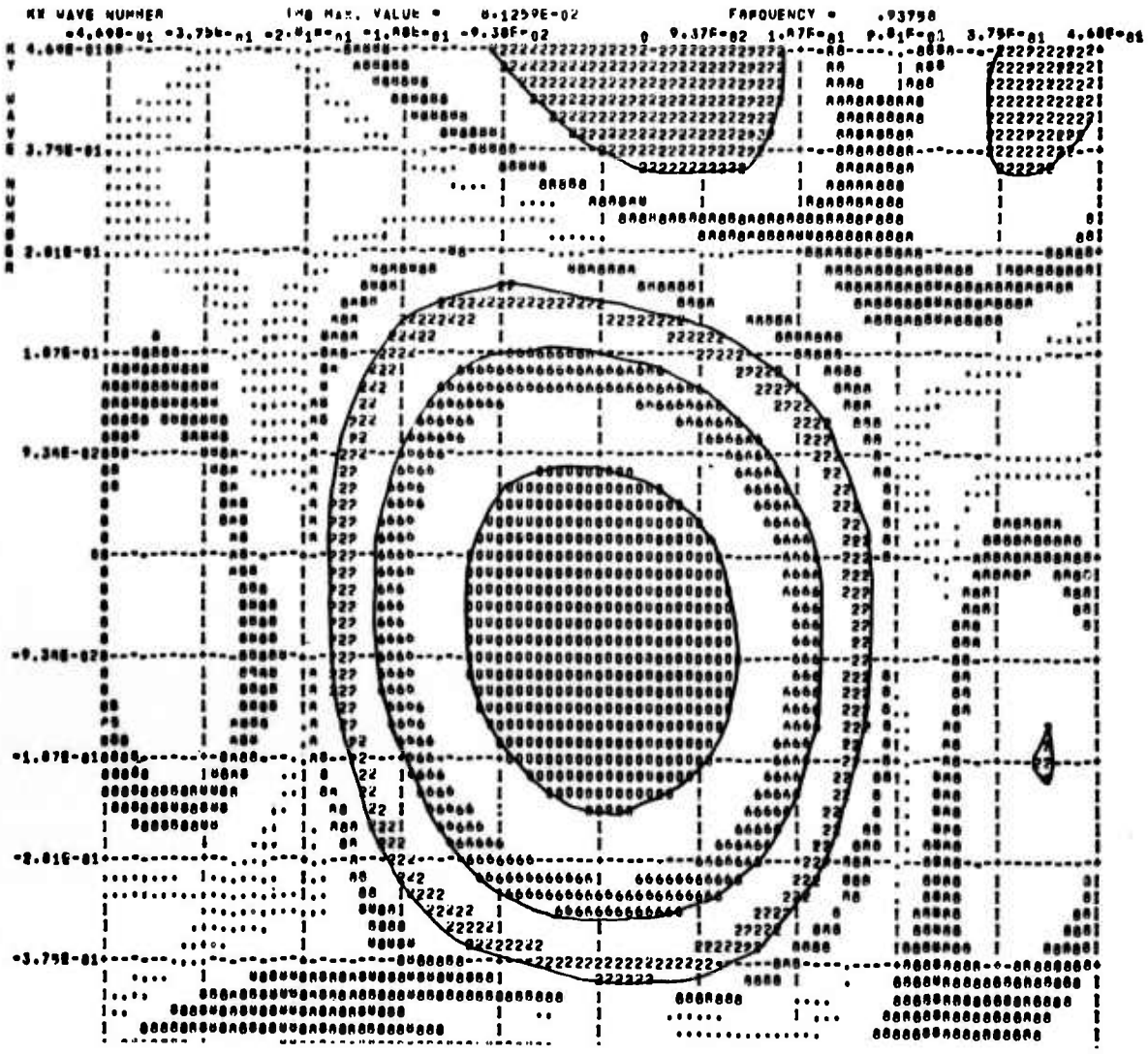

Figure 7. The ordinary f-k spectrum for the 12 km/sec plane wave at .9375 cps.

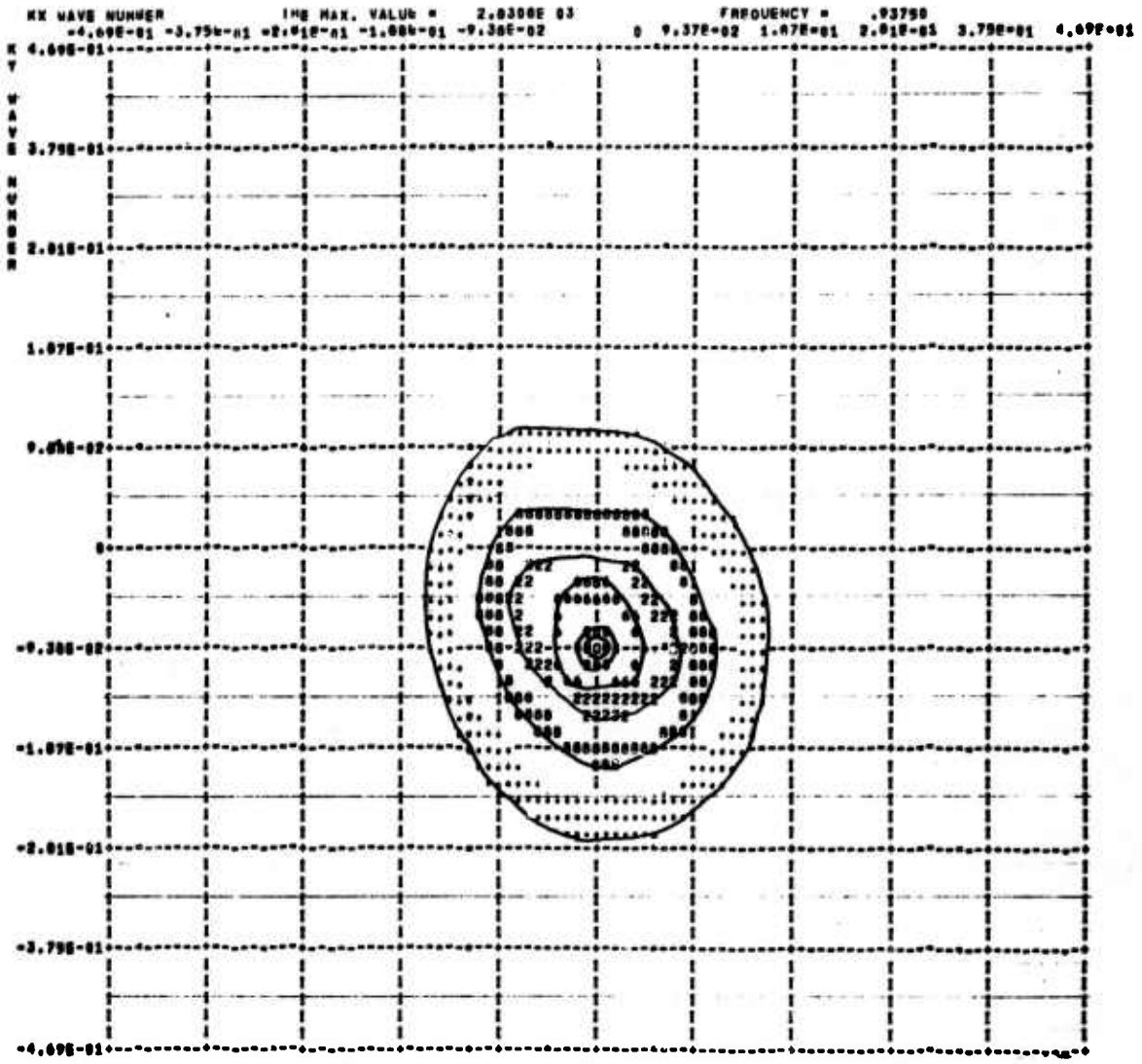

Figure 8. The High-resolution f-k spectrum for the 12 km/sec plane wave at .9375 cps. The reference seismometer was at the origin; S/N = .03.

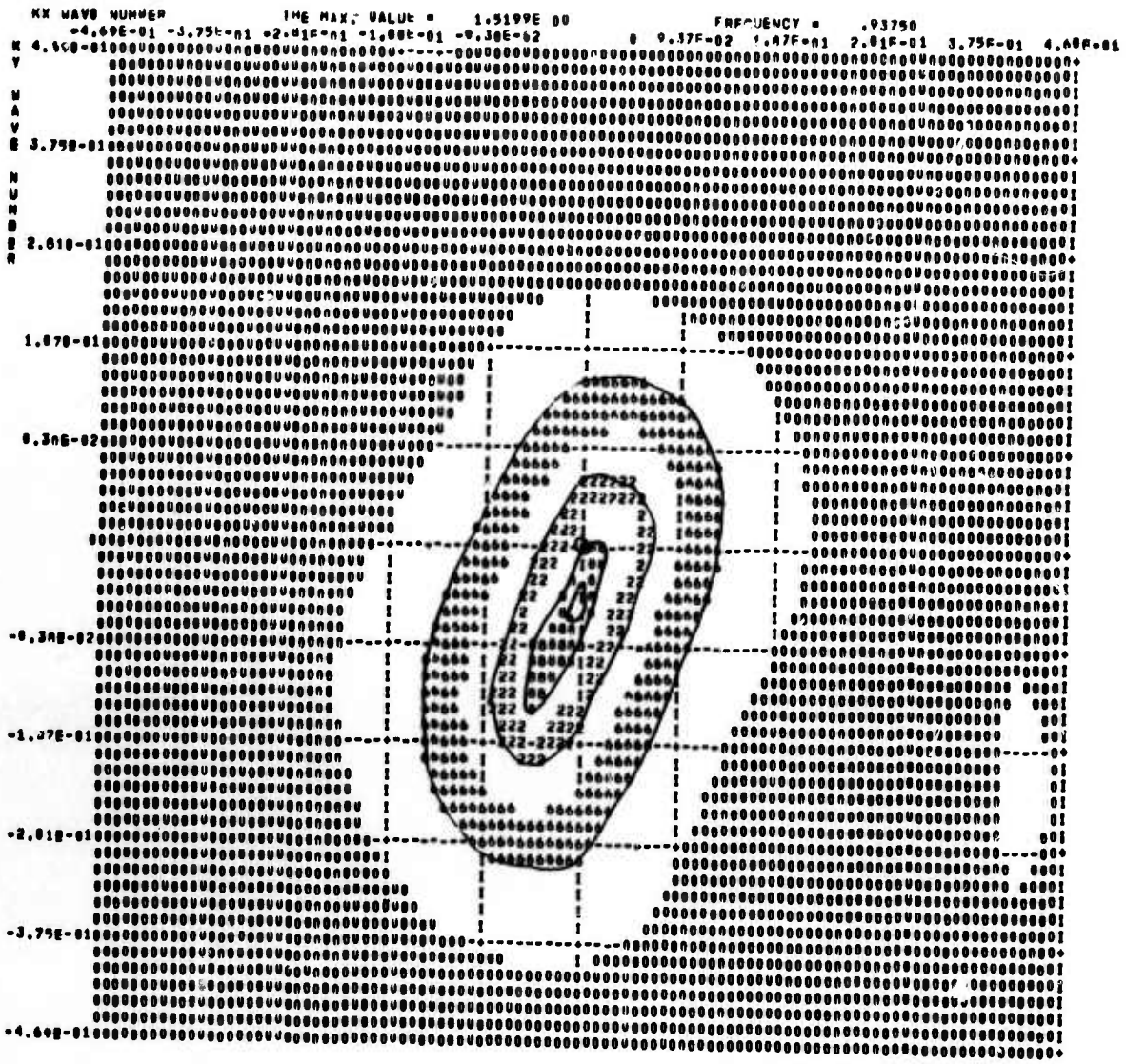

Figure 9. The high-resolution f-k spectrum for the 12 km/sec plane wave at .9375 cps. Reference seismometer (.94,-.17); S/N = .03.

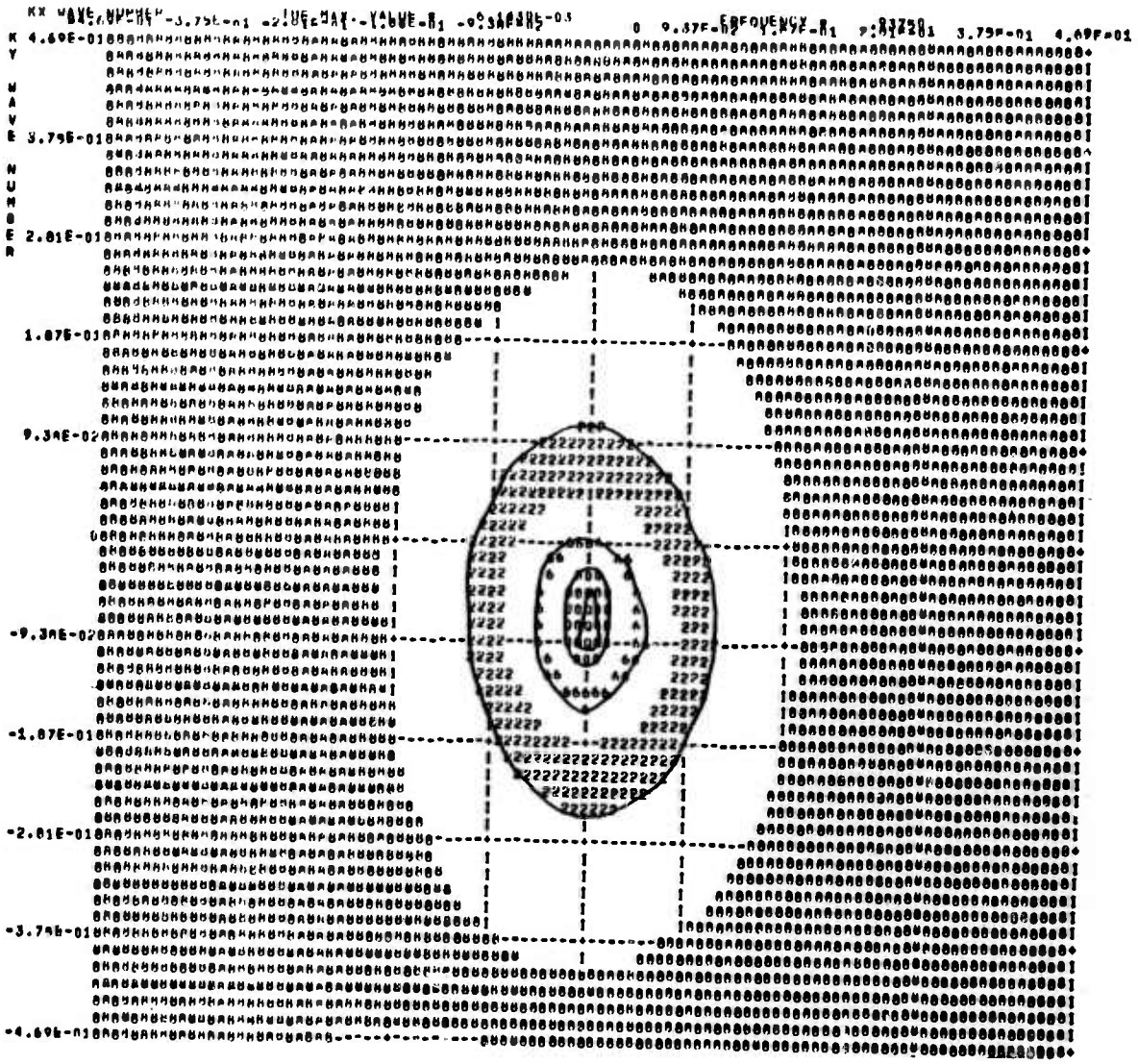

Figure 10. The high-resolution wavenumber spectrum of the 12 km/sec plane wave at .9375 cps. The spectrum was averaged over all of the seismometers in the array.

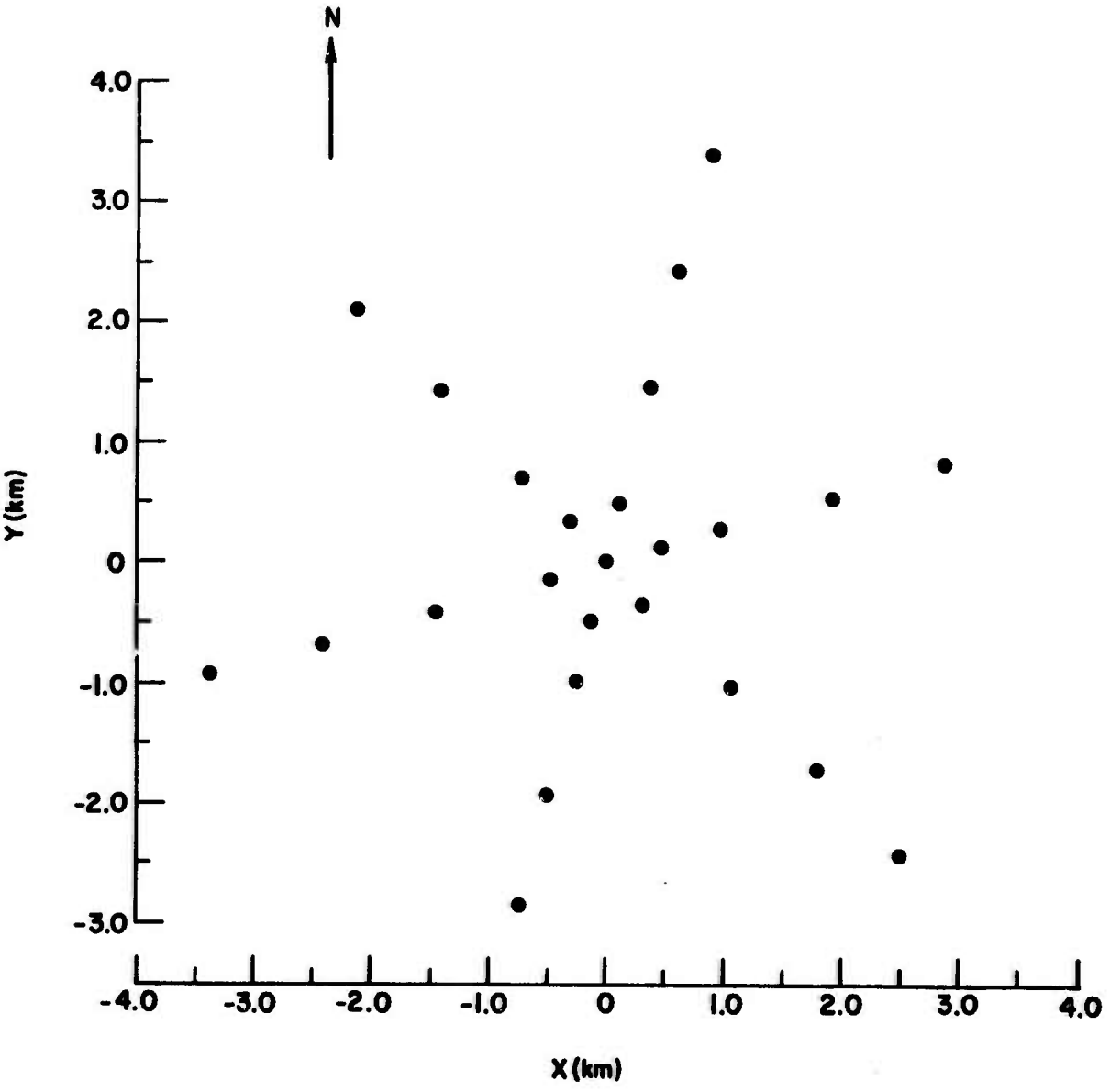

Figure 11. A map of the LASA subarray F1 seismometer grid.

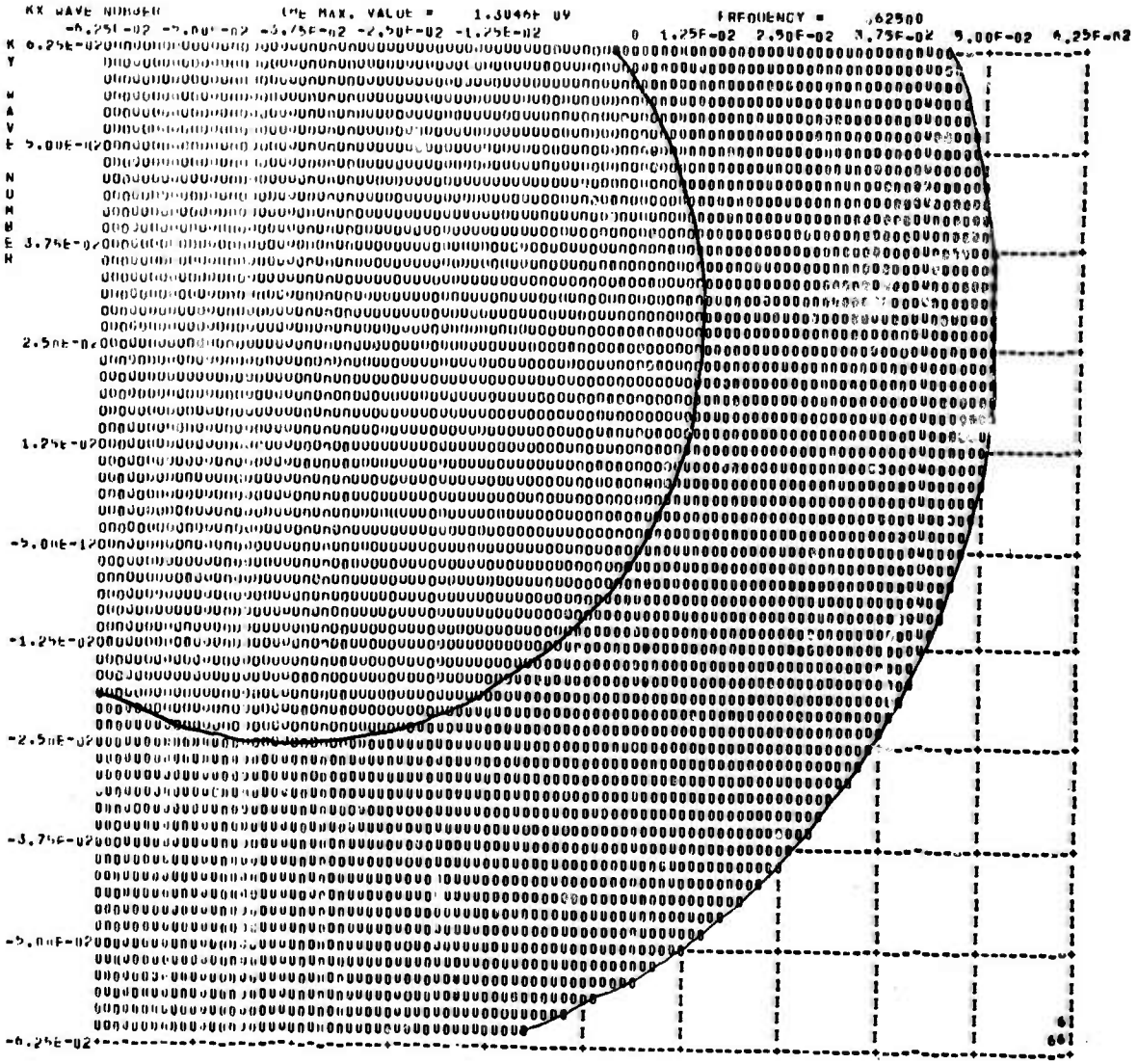

Figure 12. Ordinary f-k spectrum of LONG SHOT at LASA sub-array F1 at .625 cps.

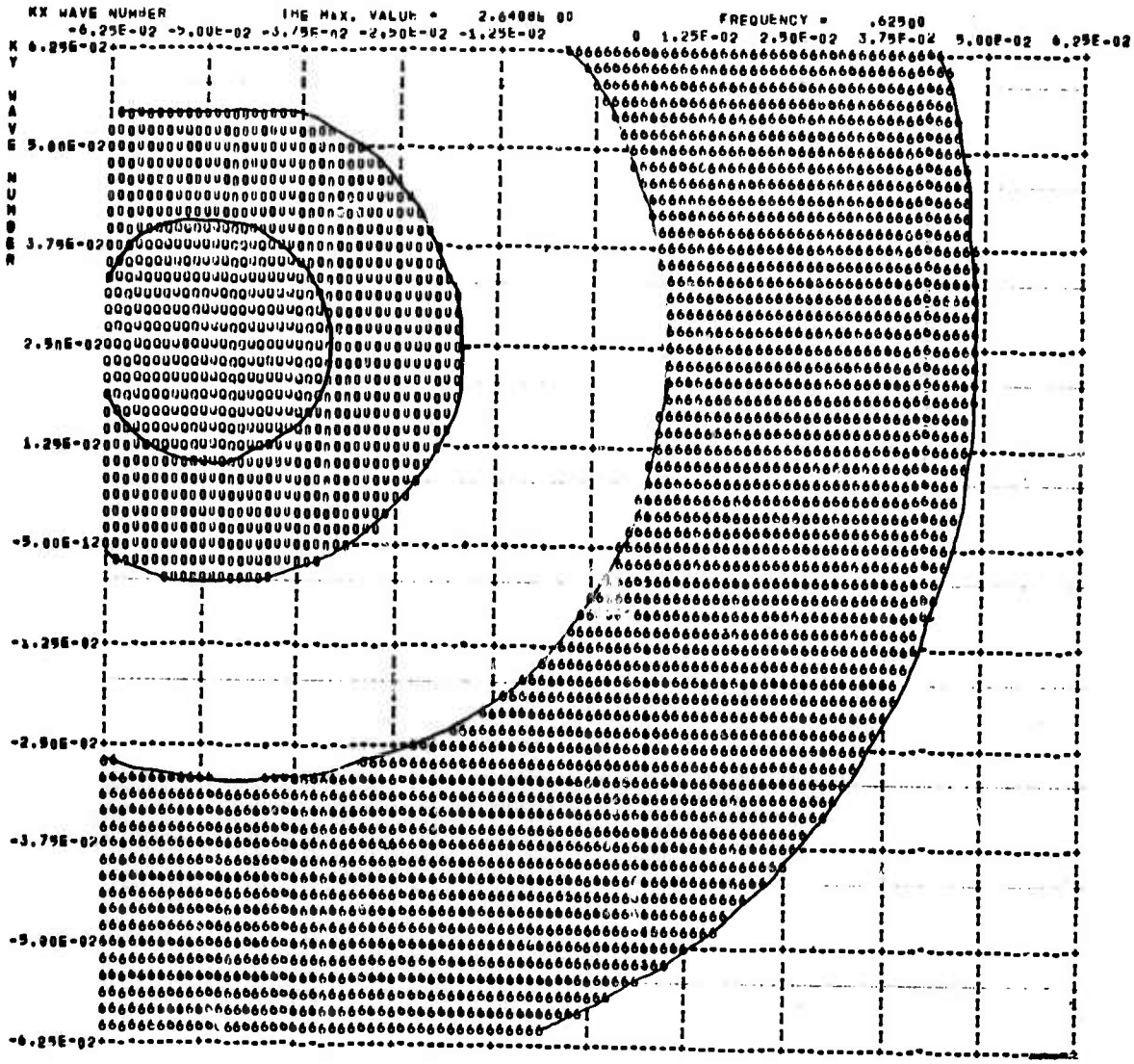

Figure 13. High-resolution f-k spectrum of LONG SHOT at LASA, F1, averaged over all seismometers in the array at .625 cps. C= 2.0.

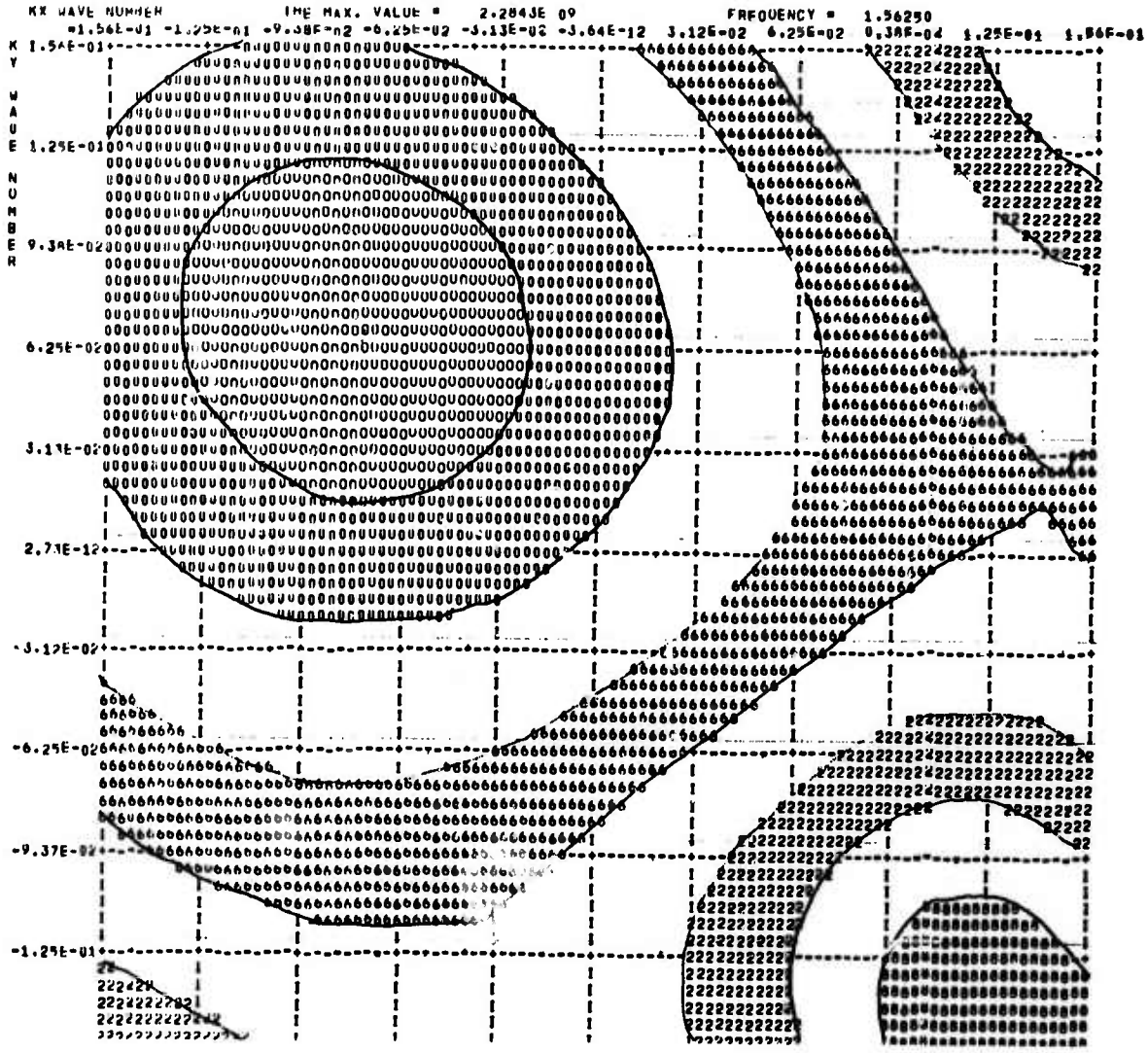

Figure 14. The ordinary f-k spectrum of LONG SHOT at LASA F1 at 1.5625 cps.

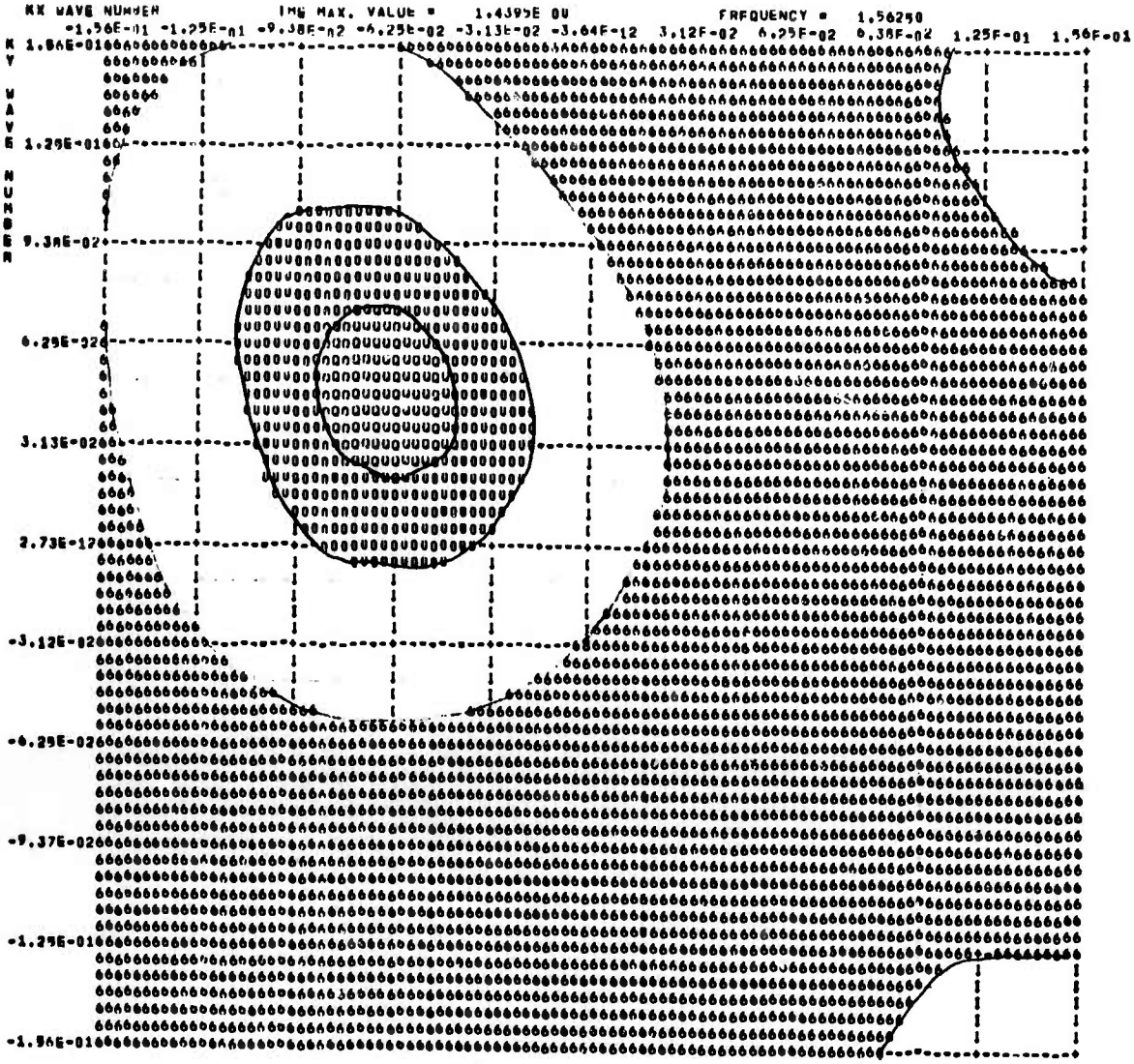

Figure 15. The high-resolution f-k spectrum of LONG SHOT at LASA F1 averaged over all of the seismometers in the array at 1.5625 cps C = 2.0.

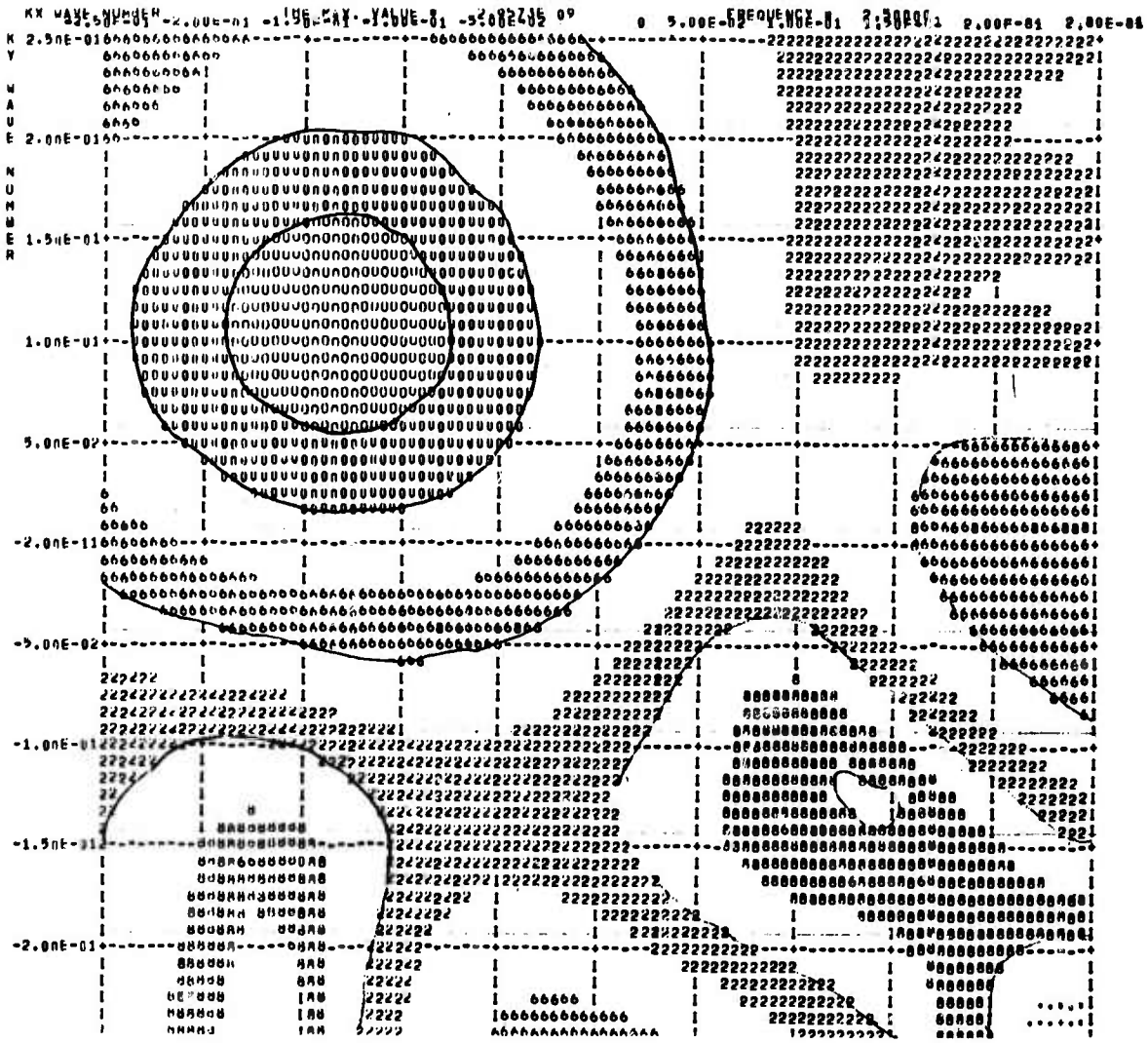

Figure 16. The ordinary f-k spectrum of LONG SHOT at LASA F1 at 2.50 cps. C = 2.0.

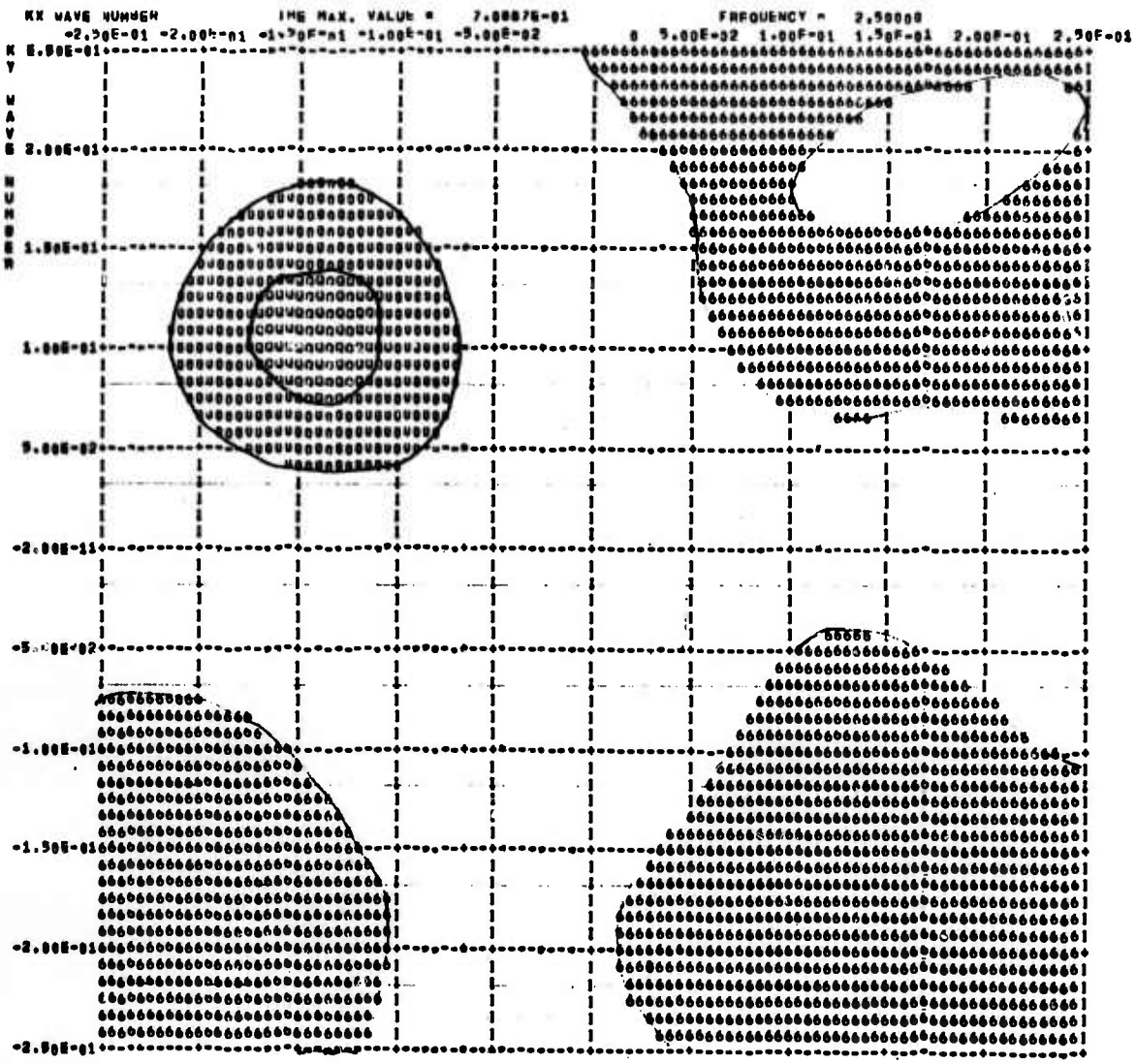

Figure 17. The high-resolution f-k spectrum of LONG SHOT at LASA F1 averaged over all of the seismometers in the array at 2.50 cps. C = 2.0.

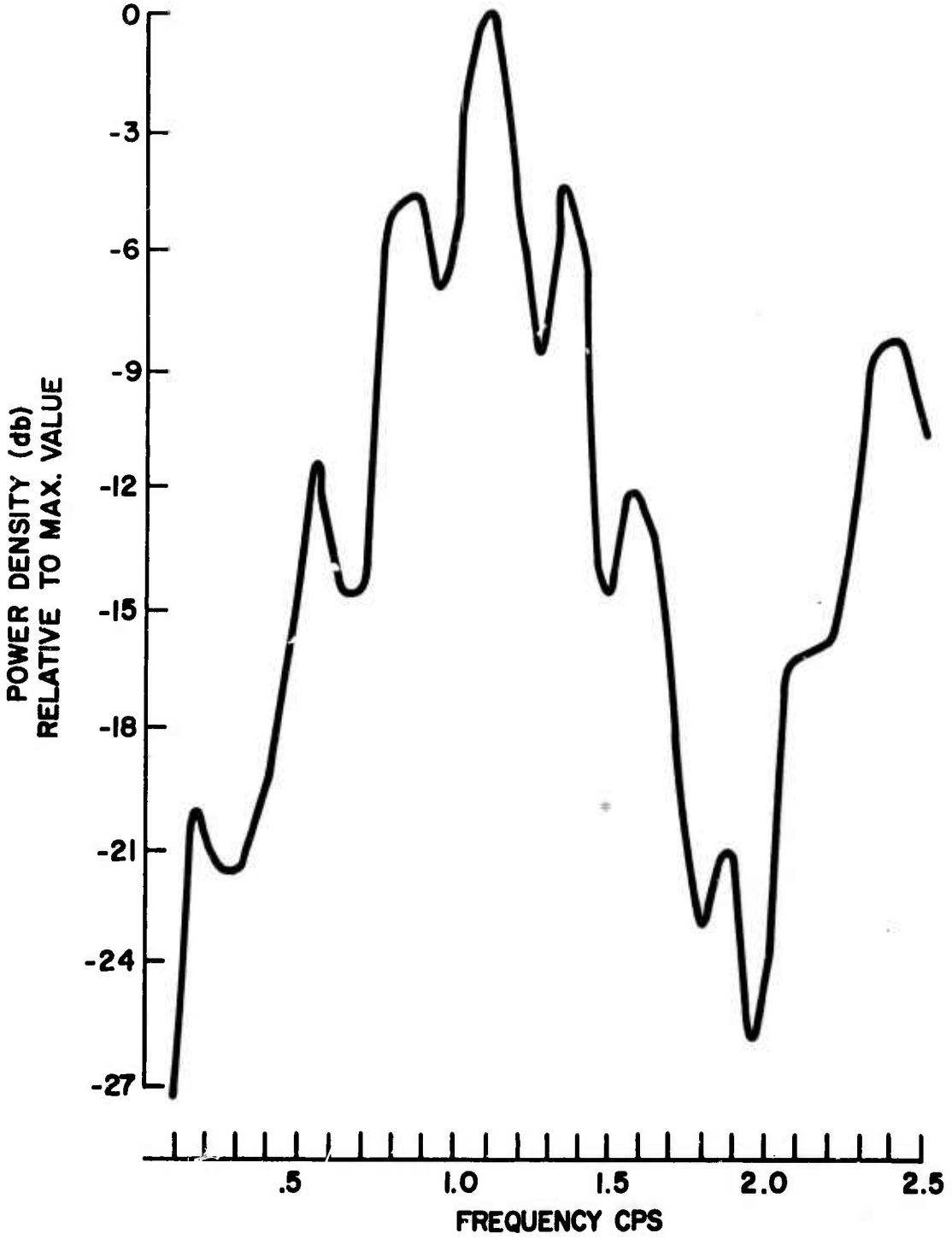

Figure 18. Beam-steered power-density spectrum of the LONG SHOT event at LASA F1.

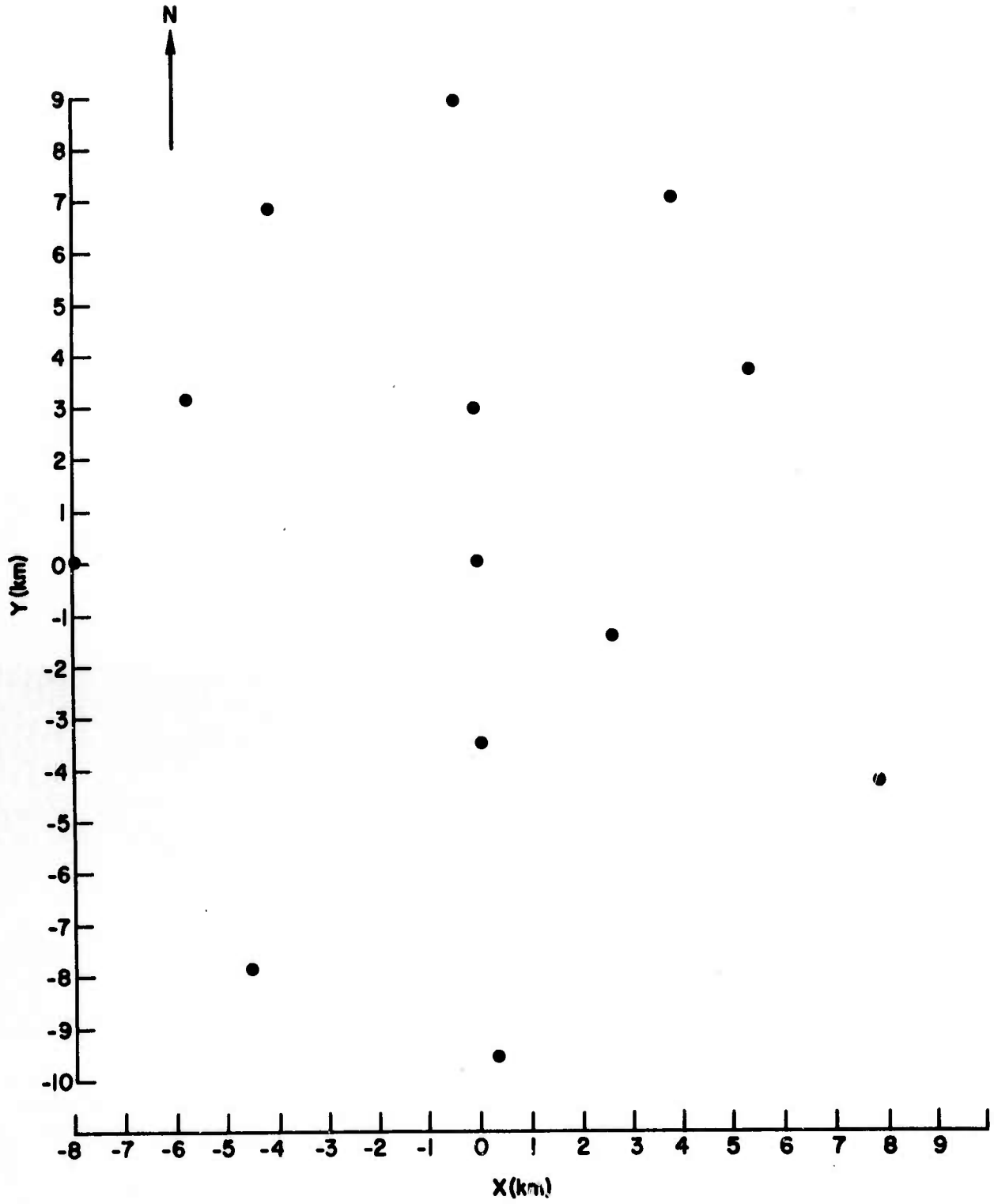

Figure 19. 13 sensors from the LASA XE3 subarray.

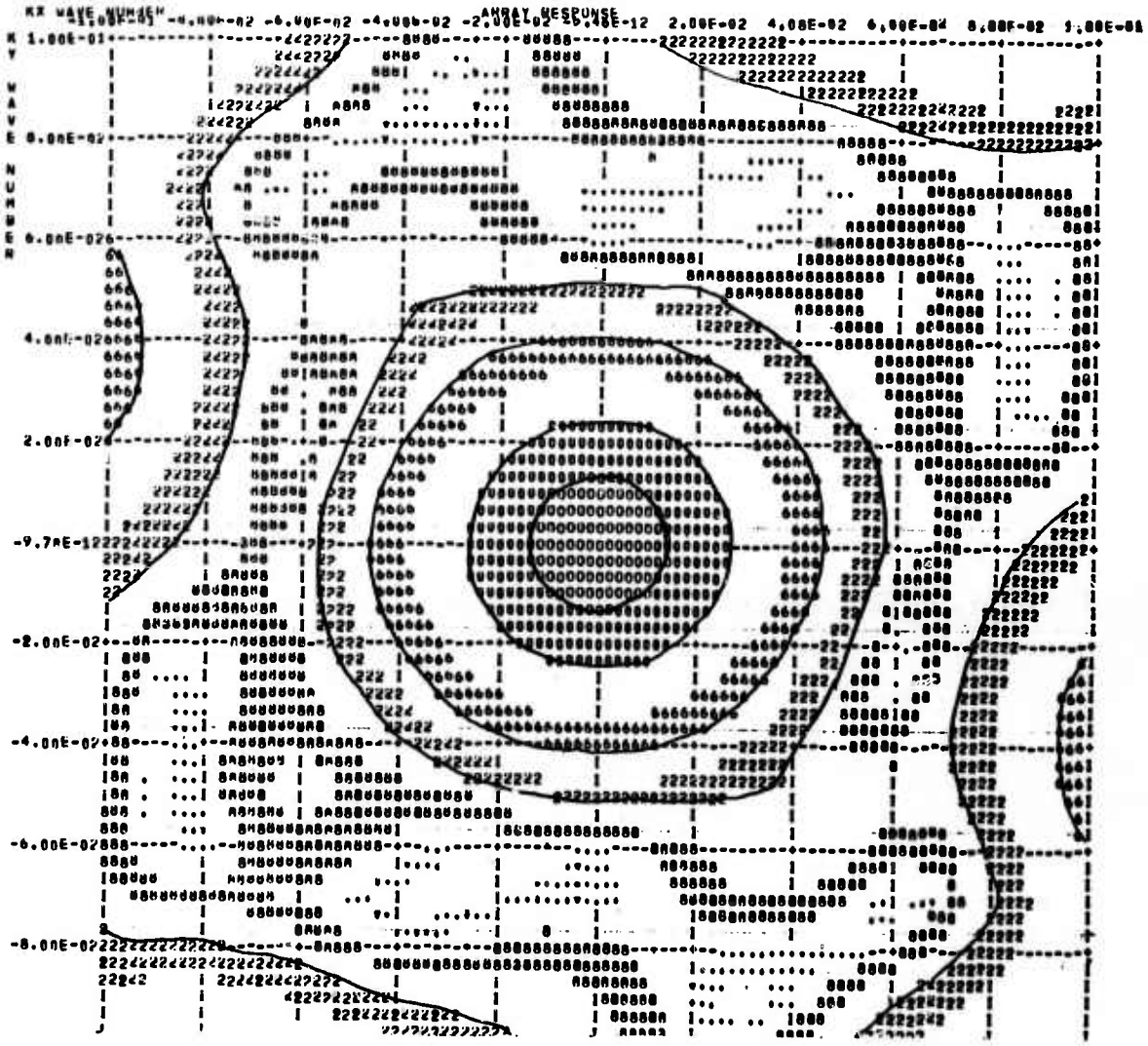

Figure 20. Array response of the partial XE3 array to an infinite velocity plane wave.

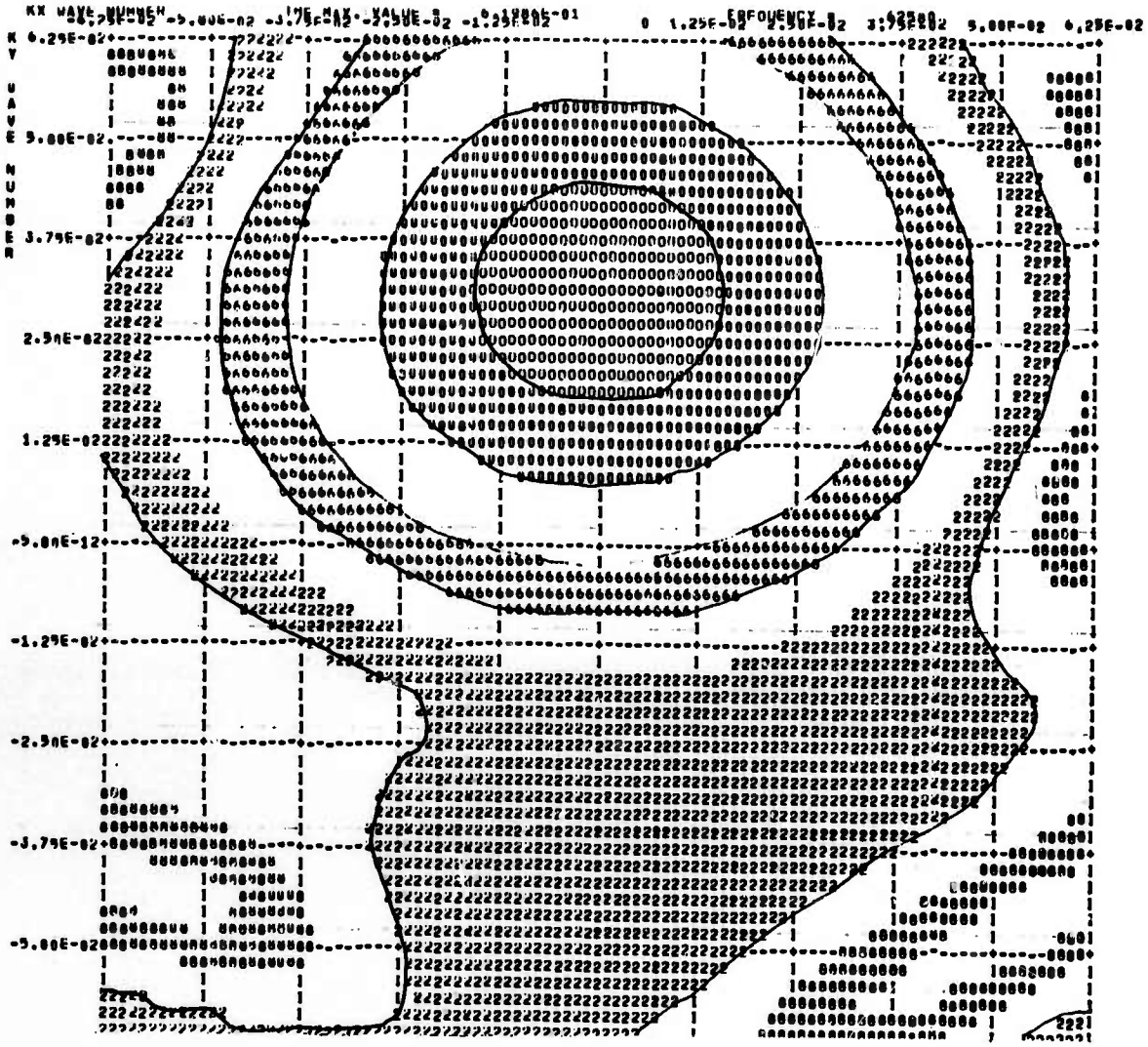

Figure 21. Ordinary f-k spectrum at .625 cps of two plane waves, one of amplitude 1 at 20 km/sec, North; and one of amplitude .2 at 30 km/sec, South.

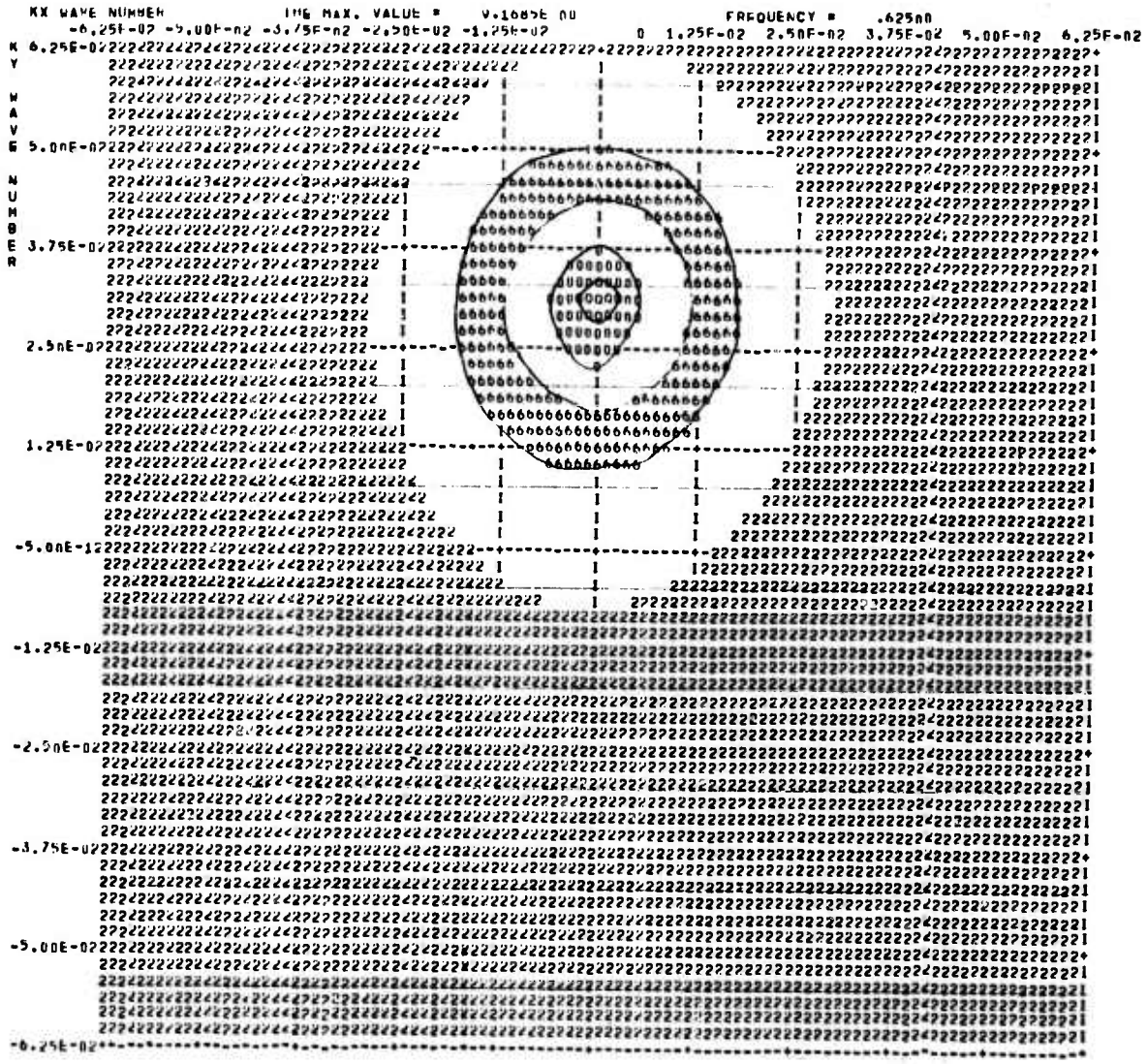

Figure 22. High-resolution wavenumber-spectrum of the two plane waves at .625 cps averaged over all of the sensors in the array S/N = 2.0.

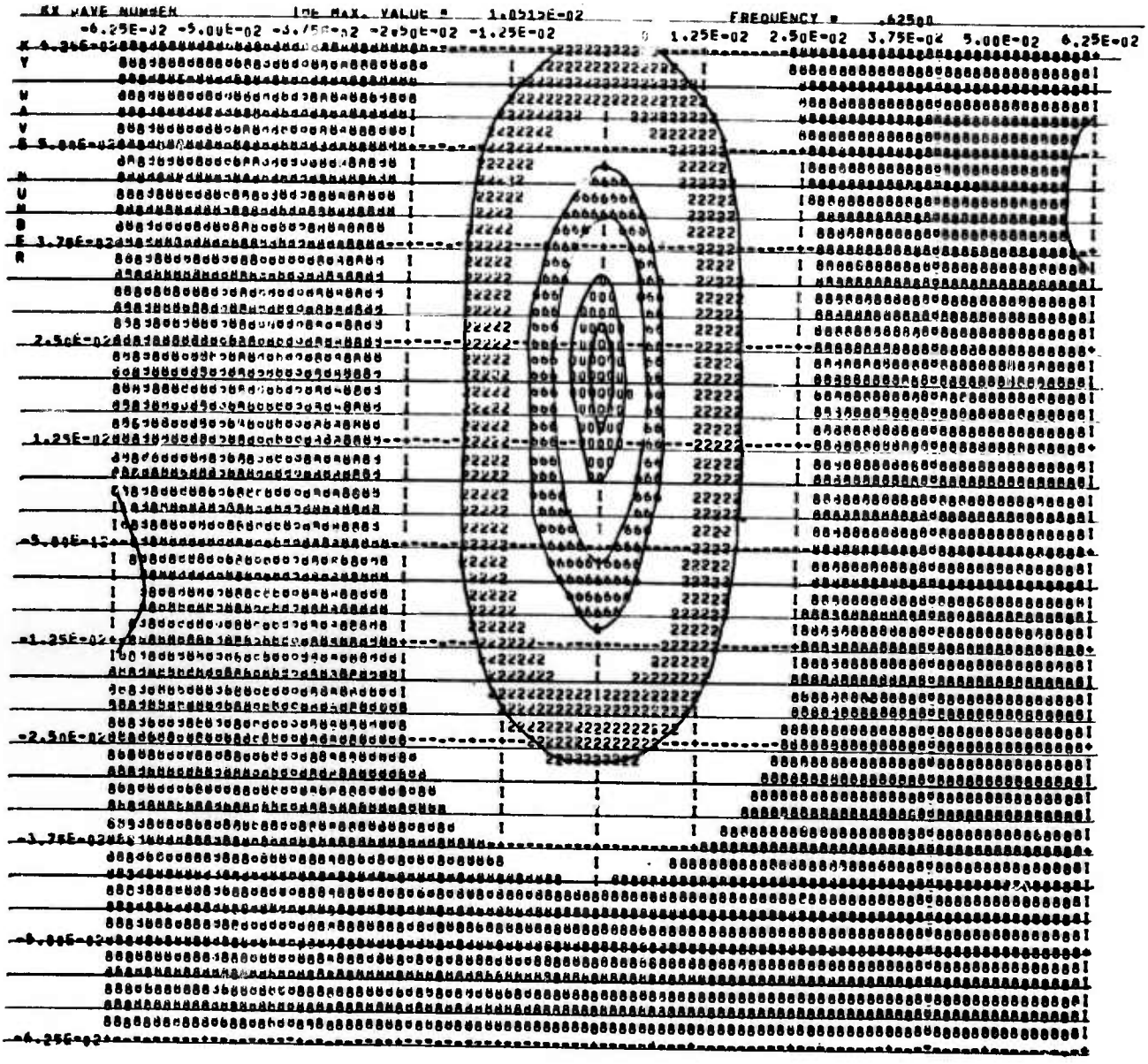

Figure 23. High-resolution wavenumber spectrum of the two plane waves at .625 cps averaged over all of the sensors in the array. S/N = .03.

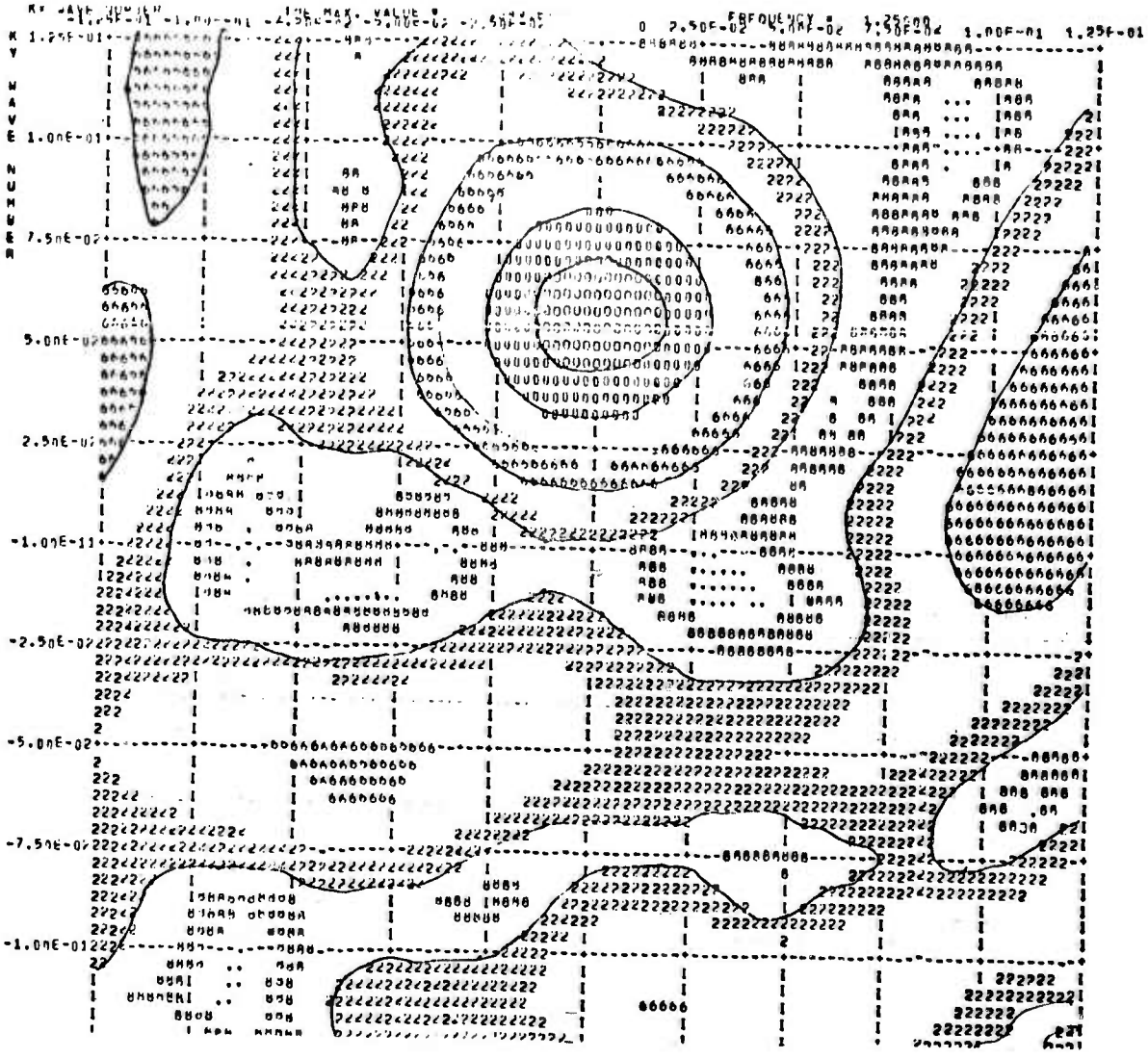

Figure 24. Ordinary f-k spectrum of the two plane waves at 1.25 cps.

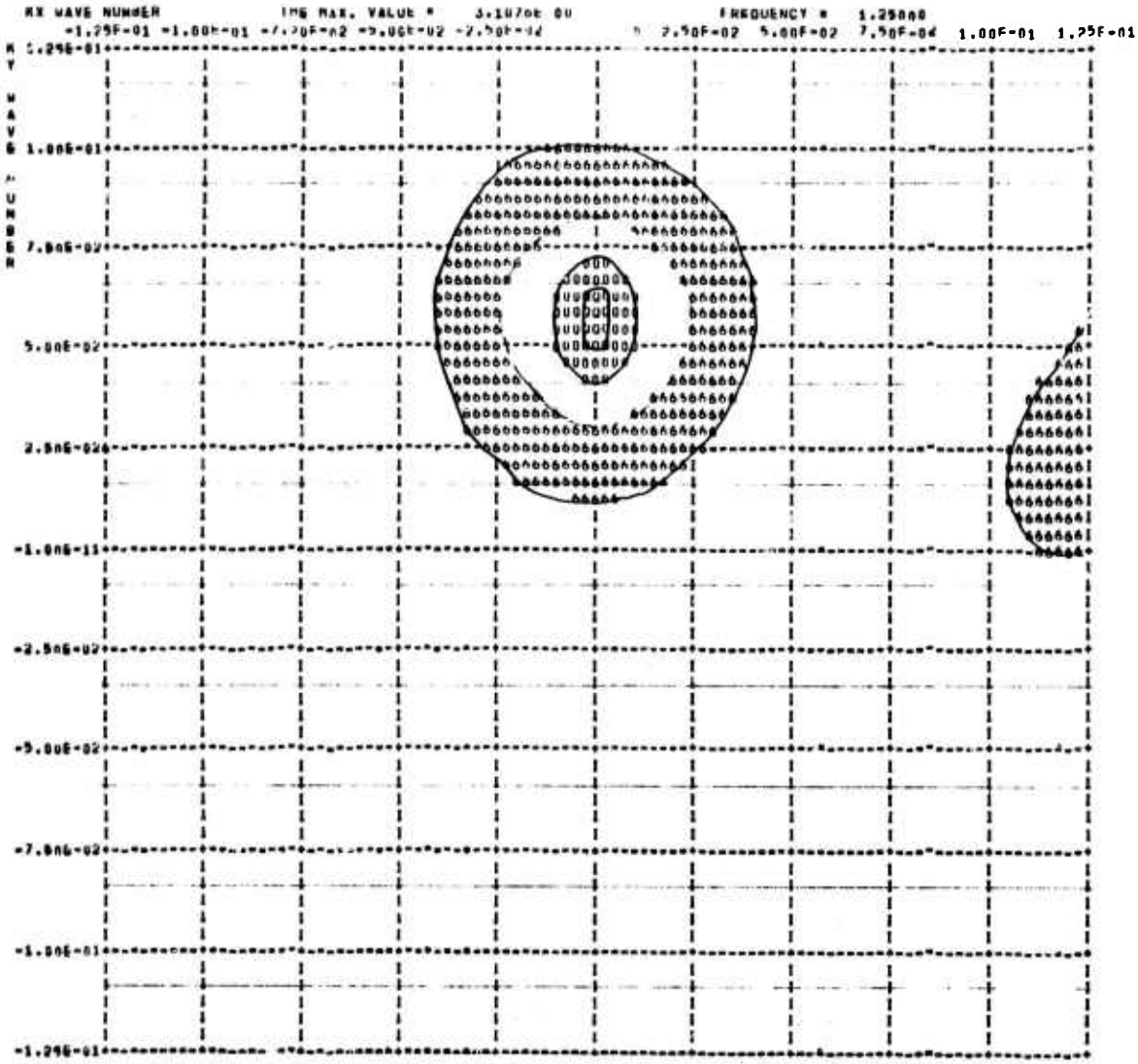

Figure 25. High-resolution f-k spectrum of the two plane waves at 1.25 cps averaged over all of the seismometers in the array. S/N = 2.0.

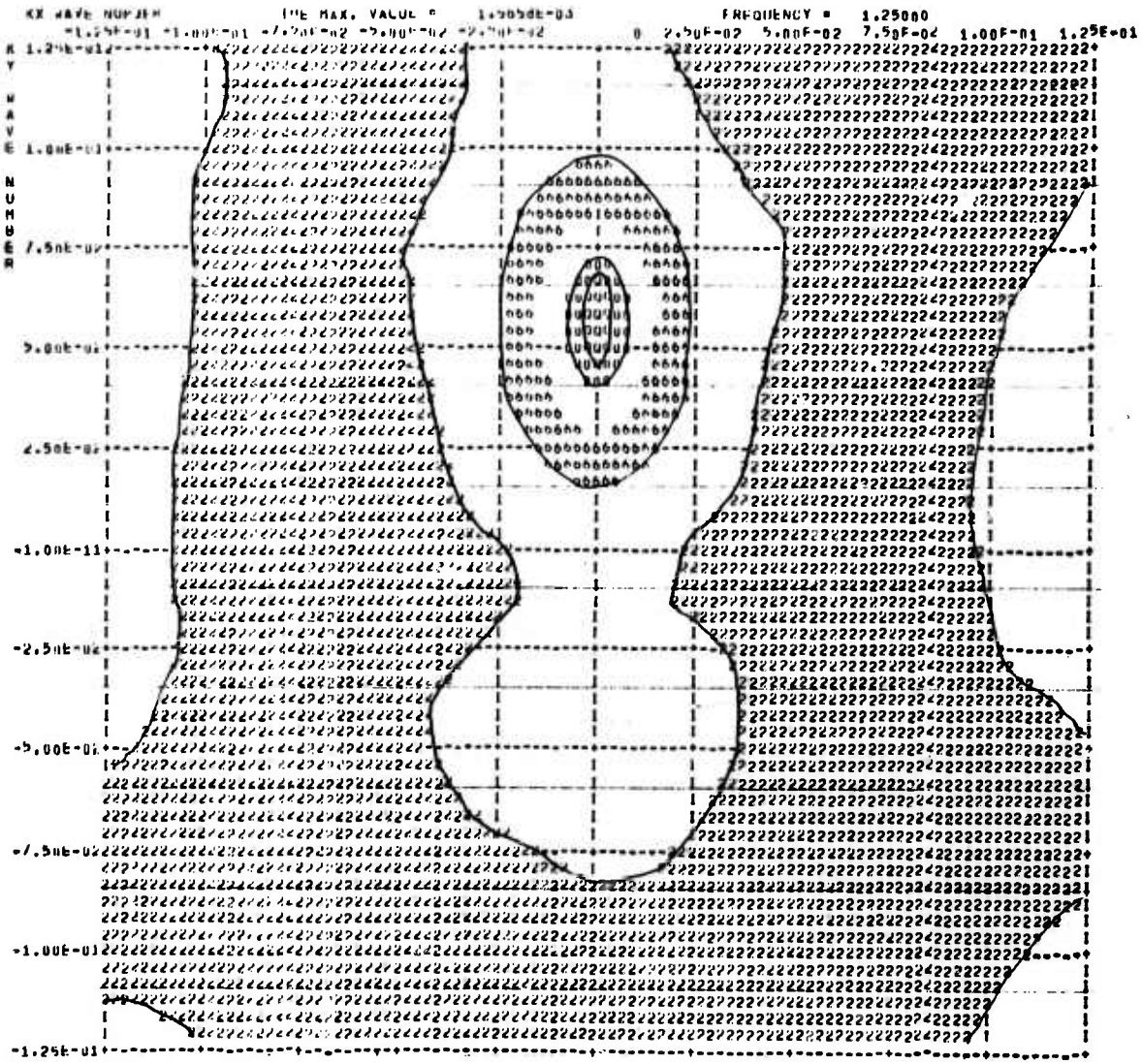

Figure 26. High-resolution f-k spectrum of the two plane waves at 1.25 cps averaged over all of the seismometers in the array. S/N = .03.

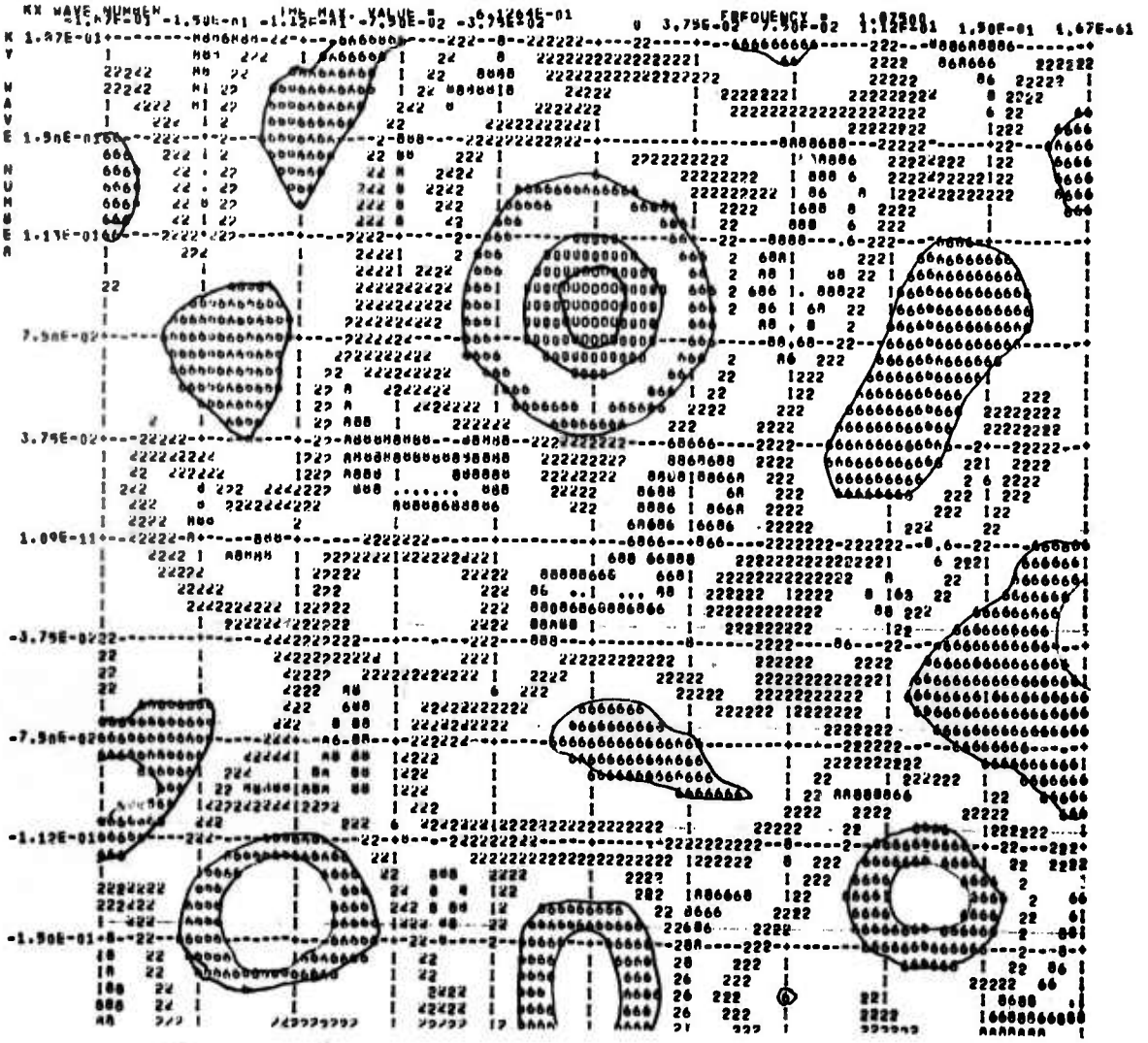

Figure 27. The ordinary f-k spectrum of the two plane waves at 1.875 cps.

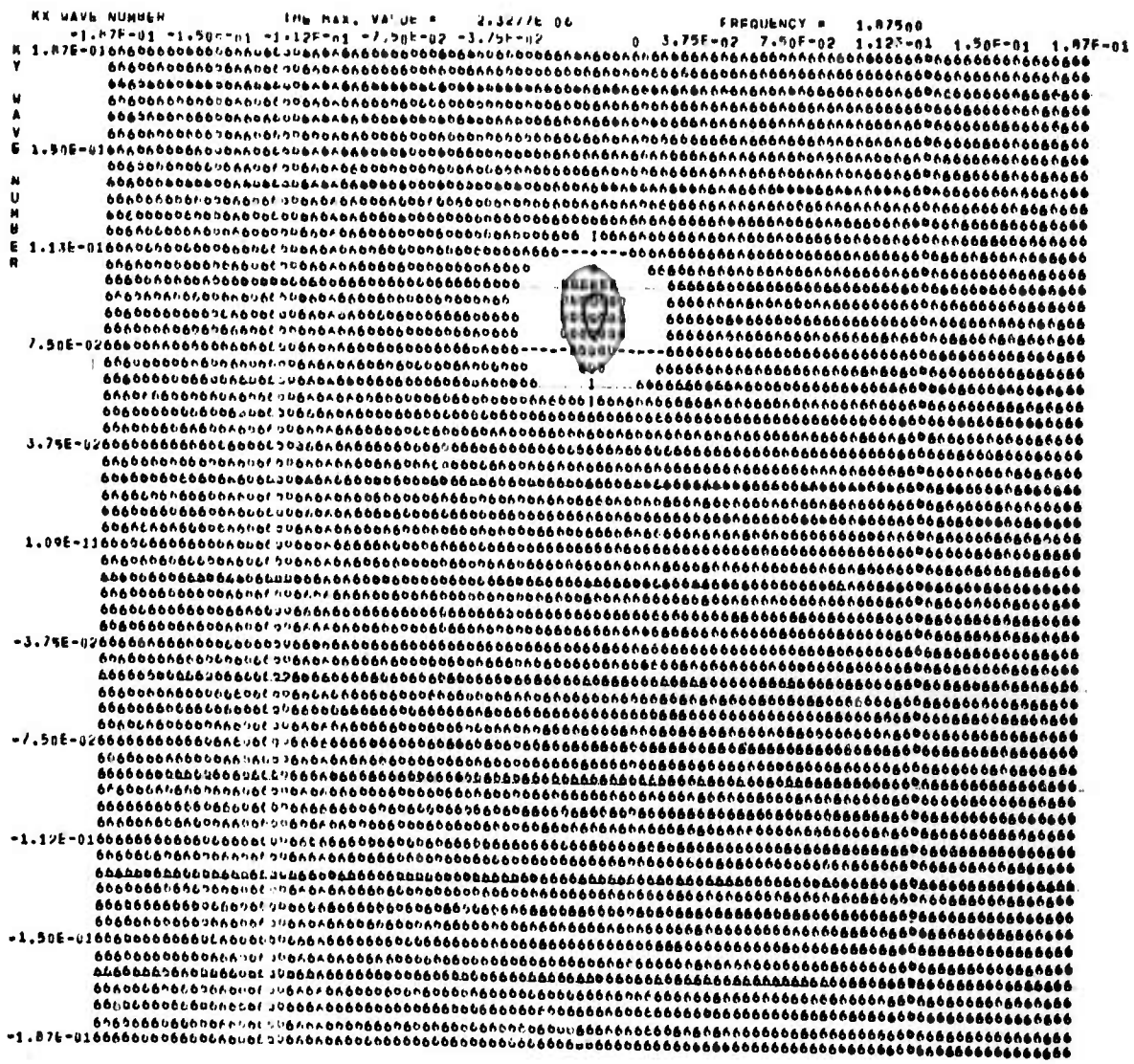

Figure 28. The high-resolution f-k spectrum of the two plane waves at 1.875 cps, averaged over all of the seismometers in the array S/N = 2.0.

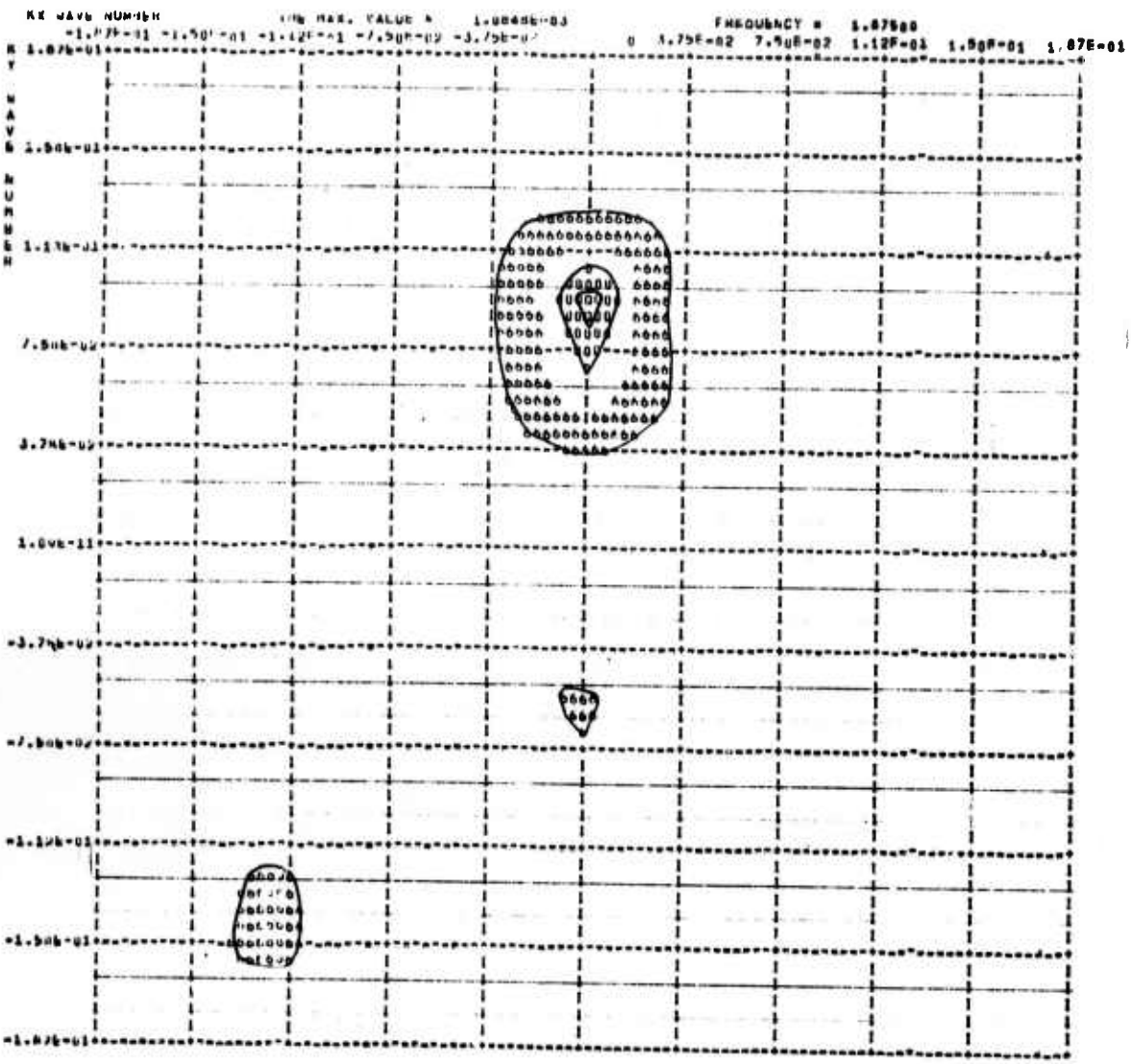

Figure 29. The high-resolution wavenumber spectrum of the two plane waves at 1.875 cps, averaged over all of the sensors in the array. C = .03.

Unclassified

Security Classification

DOCUMENT CONTROL DATA - R&D

(Security classification of title, body of abstract and indexing annotation must be entered when the overall report is classified)

1. ORIGINATING ACTIVITY (Corporate author)

TELEDYNE INDUSTRIES, INC.
ALEXANDRIA, VIRGINA 22314

2a. REPORT SECURITY CLASSIFICATION

Unclassified

2b. GROUP

3. REPORT TITLE

AN ANALYSIS OF A TECHNIQUE FOR THE GENERATION OF HIGH RESOLUTION WAVENUMBER SPECTRA

4. DESCRIPTIVE NOTES (Type of report and inclusive dates)

Scientific

5. AUTHOR(S) (Last name, first name, initial)

Lintz, P.R.

6. REPORT DATE	7a. TOTAL NO. OF PAGES	7b. NO. OF REFS
23 May 1968	48	5

8a. CONTRACT OR GRANT NO.	9a. ORIGINATOR'S REPORT NUMBER(S)
F 33657-68-C-0945	218
b. PROJECT NO. VELA T/6702	
c. ARPA Order No. 624	9b. OTHER REPORT NO(S) (Any other numbers that may be assigned this report)
d. ARPA Program Code No. 8F10	

10. AVAILABILITY/LIMITATION NOTICES

This document is subject to special export controls and each transmittal to foreign governments or foreign nationals may be made only with prior approval of Chief, AFTAC.

11. SUPPLEMENTARY NOTES

12. SPONSORING MILITARY ACTIVITY

ADVANCED RESEARCH PROJECTS AGENCY
NUCLEAR TEST DETECTION OFFICE
WASHINGTON, D.C.

13. ABSTRACT

In this report, we discuss a method of obtaining a high-resolution wavenumber spectrum of time series data obtained from a seismic array. We derive the theoretical high-resolution wavenumber spectrum of both a single plane-wave event and an event made up of the sum of two plane waves of different amplitudes. We then process the two theoretical events and analyze the results. The plane waves for both events are simulated by impulses, with time delays between sensors chosen to simulate move out across the array. We also process the LONG SHOT event.

We conclude that although the high-resolution wavenumber spectrum does indeed give better resolution than the ordinary wavenumber spectrum, the high-resolution technique does not do a much better job of detecting a small signal in the presence of a large signal than the ordinary wavenumber spectrum. It appears that the problems of detecting a small signal in the presence of a large signal might be approached by designing an "approximate" k-space whitening filter in the time domain to "pre-whiten" the data in k-space, and then to proceed with ordinary or high-resolution frequency-wavenumber analysis.

14. KEY WORDS

High Resolution Wavenumber Spectra

Frequency-Wavenumber Spectra

K-Space Whitening Filter

Spectral Matrix

Unclassified

Security Classification